Molecular Bonding and Interactions at Aqueous Surfaces as Probed by Vibrational Sum Frequency Spectroscopy

G. L. Richmond

Department of Chemistry, University of Oregon, Eugene, Oregon 97403

Received September 25, 2001

Contents

Geraldine Richmond holds the Richard M. and Patricia H. Noyes Professor of Chemistry position at the University of Oregon. She received her Ph.D. degree under the mentorship of George Pimentel at the University of California, Berkeley, in 1980. From 1980 to 1985 she was on the faculty at Bryn Mawr College and moved to the University of Oregon in 1985 as an associate professor. Richmond is recognized for her fundamental studies of the structure, dynamics, and bonding characteristics of surfaces and interfaces. Her research group uses a combination of linear and nonlinear optical methods, thermodynamic measurements, and theory to characterize interactions at aqueous surfaces, metal and semiconductor surfaces in contact with liquids and adsorbates, and liquid/liquid interfaces. Richmond has received several recent honors for these studies including the 2002 ACS Spectrochemical Analysis Award, the 2001 Oregon Scientist of the Year, and the 1996 Olin-Garvan Medal of the ACS and has been a Fellow of the American Physical Society since 1993.

I. Introduction

Aqueous surfaces and interfaces are important in many physical, chemical, and biological processes in our world. The adsorption, dissolution, and reaction of atmospheric gases at the surfaces of atmospheric aerosols and oceanic waters play a key role in the composition of our atmosphere and the sustainability of plant and animal species in land waters. The transport and exchange of ions and solutes across the interface between an aqueous phase and hydrophobic biomolecular assemblies underlies some of the most important processes in living plants and animals. Membrane formation, protein folding, and micelle formation all involve, and are often controlled by, bonding interactions with water molecules at their surfaces. The unique physical, chemical, and biological properties of aqueous surfaces arise from the strong hydrogen bonding that occurs between water molecules and the asymmetry in this otherwise tetrahedral bonding coordination that results from the termination of the bulk water phase. Although there has been increased experimental and theoretical effort in recent years focused on developing a molecular picture of the structure and bonding of water layers to other solid, liquid, and gaseous media, consensus on the details of interfacial bonding has been slow or nonexistent in many areas. The adsorption of ions, surfactants, and solute molecules at these interfaces adds a level of complexity to the

10.1021/cr0006876 CCC: $39.75
Published on Web 07/27/2002

interfacial picture that is only beginning to be addressed in molecular level experimental and theoretical efforts.

A major factor in the slow progress made in understanding hydrogen bonding and adsorption at aqueous surfaces is the paucity of experimental studies that selectively probe in situ these aqueous surfaces and interfaces. In the realm of surface science, the field is in the dark ages relative to what we know about adsorption of molecules on solid surfaces under more controlled vacuum conditions. Much of the progress for aqueous surfaces has come from theoretical efforts over the past several decades,[1−15] but even these studies are limited to relatively simple descriptions of the interactions between water molecules, solutes, and adsorbates at aqueous surfaces. It is clear that the challenge to fully understand surface water hydrogen bonding and adsorption at aqueous interfaces will continue into the future due to the complexity of interactions possible at these interfaces. However, the challenge is worth pursuing with vigor because of the central role that aqueous surfaces play in all aspects of our atmospheric and oceanic environment, in the most important biochemical processes in our body including respiration, ion transport, and protein folding, and in technological areas that range from oil extraction to semiconductor processing.

What is clearly needed in order to make progress in this area are more experimental studies of these interfaces that can selectively probe the interfacial region and coupling of these experimental studies with theoretical efforts. Recent advances in a number of newly developed experimental techniques for specifically studying liquid surfaces bode well for the future.[16−32] The focus of this review is on the contribution of vibrational sum frequency spectroscopy (VSFS) to our understanding of the bonding and structure at aqueous surfaces.[33] As a relatively new vibrational spectroscopic method, it is showing particular promise for measuring the molecular spectroscopy of water and adsorbed molecules at liquid interfaces because of its inherent ability to discriminate between molecules that reside in that thin molecular layer that defines a surface and those molecules in the centrosymmetric bulk media. Whereas a decade ago the technique was used only by a handful of investigators, its use is rapidly growing as more investigators are discovering the unique information that can be gained from its applicability to a wide range of systems. This review provides an overview of the studies that have thus far employed VSFS to study aqueous surfaces and interfaces, with a particular focus on the structure and hydrogen bonding of water at the surface of neat water and aqueous solutions studied at the vapor/water interface and the interface between two immiscible liquids (organic/water interface). It highlights many of the recent studies in the field as a means of demonstrating the type of information obtainable. In addition, it seeks to provide the reader with a sense of where future development is needed in the technique and analysis methods in order for VSFS to reach the general applicability as a vibrational spectroscopic method that vibrational infrared (IR) and Raman spectroscopies have attained.

The article begins with a description of the technique, conceptual underpinnings, experimental considerations, and issues that must be considered in the analysis of VSF data. This is followed by a section that focuses on VSF studies of the neat vapor/water interface. The neat vapor/water interface is one of the simplest systems to examine from a chemical perspective, and yet there are many unknowns about the molecular structure and bonding at this interface and the related vapor/ice interface. This is followed by an overview of what has been learned through VSF studies about water structure hydrogen bonding at an interface between water and an immiscible liquid, referred to as the organic/water interface. As will be shown, there are distinct differences and similarities in the nature of hydrogen bonding at these two interfaces that will play an important role in our understanding of many processes in living organisms and in our environment. Water structuring next to a hydrophobic surface is central to issues of wettability, protein folding, chemical separations, and oil extraction—to name only a few. Beyond these neat water surface studies, this review will examine how the hydrogen bonding at water surfaces is altered by the presence of surfactants at the surface and by variation of the composition of the aqueous phase by addition of salts, acids, and bases.

The second portion of the review examines the molecular structure of adsorbates at aqueous surfaces. This is divided into two parts: the first focuses on small solute molecules adsorbed at aqueous surfaces, with atmospherically important molecules being the most prevalent systems examined. In these studies the molecular orientation and bonding of sulfur- and nitrogen-containing solutes have been examined. The second part discusses VSF studies of alkyl surfactants adsorbed at both the vapor/water and organic/water interfaces. A wide variety of commercially important surfactants have been examined in these studies with the primary focus on measuring conformational ordering and orientation of alkyl portions of the surfactants. Recent studies of biological surfactants, namely, phospholipids, will also be described. Phospholipids are important components of biological membranes, and understanding their behavior at these aqueous interfaces is important for understanding a host of important biological processes.

II. Vibrational Sum Frequency Spectroscopy

A. Principles and Concepts

Vibrational spectroscopy has long been recognized as an important tool for measuring molecular structure in gases, liquids, and solids. This is as true for molecules at surfaces as it is for molecules in bulk media. Vibrational sum frequency spectroscopy is a technique that is uniquely suited for measuring the vibrational spectrum of molecules at surfaces.[33] In a VSFS experiment, light pulses from a visible laser beam and a tunable IR laser beam are coincident in time and space at the interface. Figure 1 provides

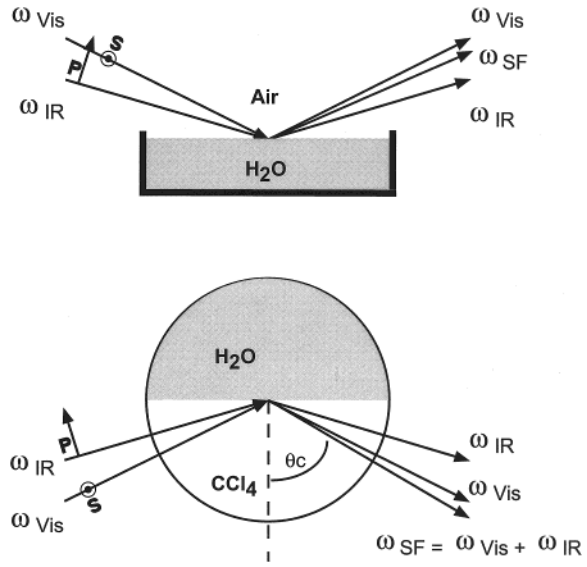

Figure 1. Schematic of the VSF method as applied to vapor/water and organic/water interfaces. *P* and *S* correspond to the polarization of the light either parallel or perpendicular to the incident plane, respectively.

an illustration of the experiment for two different systems, the vapor/water interface (above) and the liquid/liquid interface (below). The high-intensity electric fields of the incident laser beams induce a coherent nonlinear polarization in the molecules at the interface, and this oscillating nonlinear polarization at the sum of the two frequencies is the source of SF light collected. When the infrared source is tuned through the spectral region of interest, coincidence between the photon energy and the energy of the molecular vibrational mode results in a resonant enhancement in the SF response. It is similar to the optically simpler second harmonic generation (SHG) process that involves the summation of two fixed frequency light beams.[31,33−36] The surface specificity arises from the second-order nature of the response. Under the dipole approximation, this second-order response is forbidden in media possessing inversion symmetry.[34,37] At the interface between two centrosymmetric media there is no inversion center and the SF process is allowed. This inherent surface sensitivity makes it an advantageous method of studying the vibrational spectroscopy of molecules at surfaces over other linear vibrational spectroscopies such as infrared or Raman spectroscopy. The disadvantage to date over these other methods has been the difficulty in measuring VSF spectra over a broad IR frequency range (due to limitations in IR laser systems used) and the weak SF signals due to the higher order nature of the response.

The sum frequency intensity is proportional to the square of the surface nonlinear polarization. This polarization is induced by the two incident beams and gives rise to sum frequency generation; $\boldsymbol{P}_{\mathrm{SFG}}$ is dependent on the surface nonlinear susceptibility $\chi_s^{(2)}(\omega_{\mathrm{sfg}} = \omega_{\mathrm{vis}} + \omega_{ir})$ given by

$$I_{\mathrm{SFG}} \propto |\boldsymbol{P}_{\mathrm{SFG}}|^2 \propto |\chi_{\mathrm{NR}}^{(2)} + \sum_{\nu} |\chi_{\mathrm{R}\nu}^{(2)} e^{i\gamma_\nu}|^2 I_{\mathrm{Vis}} I_{\mathrm{IR}} \quad (1)$$

with $\chi_{\mathrm{NR}}^{(2)}$ and $\chi_{\mathrm{R}}^{(2)}$ the nonresonant and resonant parts of $\chi_s^{(2)}$ respectively, and γ_ν is the relative phase of the νth vibrational mode. The nonresonant part of $\chi_s^{(2)}$ depends primarily on the polarizability of the molecules at the interface and must be included in the full spectral analysis. The resonant term arises from a coincidence in frequency between the tunable infrared light and a vibrational mode in the molecule of interest. The coherent nature of the VSF response leads to a more complex expression for the sample response and a more complicated deconvolution of overlapping peaks than in linear spectroscopy. Because the nonlinear susceptibility generally has an imaginary and a real part, each resonant term in the summation is associated with a relative phase, γ_ν, which describes the interference between overlapping vibrational modes. The resonant term, $\chi_{\mathrm{R}\nu}^{(2)}$ is dependent on the number of molecules N and the orientationally averaged molecular hyperpolarizability $\langle\boldsymbol{\beta}_\nu\rangle$ in the following way

$$\chi_{\mathrm{R}\nu}^{(2)} = \frac{N}{\epsilon_{\mathrm{o}}}\langle\boldsymbol{\beta}_\nu\rangle \quad (2)$$

Given the expressions in eqs 1 and 2, the square root of the sum frequency intensity is shown to depend on the number of molecules giving rise to the response. Their average orientation can be derived through the $\boldsymbol{\beta}_\nu$ term. These two contributions can be used to determine the orientation of interfacial molecules and changes in orientation under various experimental conditions.

The enhancement in the sum frequency response that occurs when the frequency of IR radiation is resonant with a sum frequency active vibration arises from the molecular hyperpolarizability, $\boldsymbol{\beta}_\nu$. This enhancement in the molecular polarizability is given by

$$\chi_{\mathrm{R}\nu}^{(2)} \propto \frac{\boldsymbol{A}_K \boldsymbol{M}_{IJ}}{\omega_\nu - \omega_{\mathrm{ir}} - i\Gamma_\nu} \quad (3)$$

if one assumes a Lorentzian distribution of vibrational energies and that the dipole approximation holds. In this expression $\boldsymbol{A}_K$ is the IR transition moment, $\boldsymbol{M}_{IJ}$ is the Raman transition probability, ω_ν is the resonant mode frequency, and Γ_ν is the natural line width of the transition. Since sum frequency active modes must be both IR and Raman active, any molecule with an inversion center cannot be sum frequency active.

In the presence of a charge at the surface that induces an electrostatic field $\boldsymbol{E}_0$ at the interface, an additional third-order factor can contribute to the overall SF response described in eq 1. This third-order polarization term, $\boldsymbol{P}^{(3)}{}_{\mathrm{SFG}}$ takes the form of

$$\boldsymbol{P}^{(3)}{}_{\mathrm{SFG}} = \boldsymbol{\chi}^{(3)} : \boldsymbol{E}_{\mathrm{Vis}} \boldsymbol{E}_{\mathrm{IR}} \boldsymbol{E}_0 \quad (4)$$

and contains the electrostatic field dependence of the nonlinear polarization induced at the interface. This additional term has been shown to be important in a number of VSF studies where ionic species adsorb at a water surface.[38−42] The third-order contribution to the nonlinear polarization results from

several factors, namely, the electronic nonlinear polarizability, $\alpha^{(3)}$, the alignment of the interfacial water molecules by the electrostatic field $\boldsymbol{E}_o$, and the magnitude of the electrostatic field. The presence of a large electrostatic field aligns the interfacial water molecules beyond the first few water layers and thus removes the centrosymmetry over this region, thereby allowing more water molecules to contribute to the nonlinear polarization.[43]

As with any vibrational spectroscopy, spectral fitting of the data requires an appropriate choice of line shape for the vibrational peaks. The simplest approach to fitting the data is to use eq 3, which assumes a Lorentzian distribution of energies and allows for interferences between nearby vibrational modes. Unfortunately, the broad "wings" characteristic of a Lorentzian distribution often overestimate the amount of overlap, and therefore the amount of interference, between widely separated peaks. Particularly useful, although computationally more intensive, is the line shape profile described by Goates et al.[44] Similar to a Voigt profile, this line shape expression is a convolution of eq 3 and a Gaussian distribution to account for inhomogeneous broadening.[44,45] This profile is the most appropriate for the analysis of spectra exhibiting significant overlap of modes of different phases.

Although the complex nature of the nonlinear response makes data analysis more complicated relative to linear spectroscopies, the interference between different vibrations can be exploited to provide orientational information if a complete analysis of the VSF spectrum is employed that takes into account the phase relationships of the contributing vibrational modes to the sum frequency response.[46,47] In particular, it is possible to constrain the average orientation of the molecules at the surface by relating the macroscopic second-order susceptibility $\chi_{IJK,\nu}^{(2)}$ of the system to the molecular hyperpolarizabilities, $\beta_{lmn,\nu}$ of the individual molecules at the interface.[48,49] Interference effects can be understood by use of a more a rigorous expression for the molecular hyperpolarizability, $\boldsymbol{\beta}_\nu$

$$\beta_{lmn,\nu} = \frac{\langle g|\alpha_{lm}|\nu\rangle\langle\nu|\boldsymbol{\mu}_n|g\rangle}{\omega_{IR} - \omega_\nu + i\Gamma_\nu} \tag{5}$$

where l, m, and n represent the molecular inertial axes (a, b, and c); α_{lm} and $\boldsymbol{\mu}_n$ represent the Raman and dipole vibrational transition elements, respectively, for a particular vibrational mode. An energy diagram illustrating the interference between different vibrational modes is shown in Figure 2. The interference of different nearby vibrations in VSFS is analogous to the double-slit experiment. In both cases, particles passing through *indistinguishable* intermediate states give rise to distinct interference patterns.[50]

In the VSF experiment, the macroscopic observable is $\boldsymbol{\chi}_s^{(2)}$. This represents the sum of the molecular hyperpolarizabilities, $\boldsymbol{\beta}_\nu$, over all vibrational modes and all of the molecules at the interface and includes information about the orientation of each molecule. Orientational information is obtained from the experimental spectra through consideration of the relationship between the observed Cartesian components of the macroscopic second-order susceptibility $\chi_{IJK,\nu}^{(2)}$ and the corresponding spectroscopically active components of the molecular hyperpolarizability β_{lmn}. This is accomplished through an Euler angle rotation of the molecular axis system into the laboratory axis system as defined through the use of the rotational matrix $\boldsymbol{\mu}_{IJK:lmn}$. The general expression for the transformation from a molecular-fixed axis system to a laboratory-fixed system is

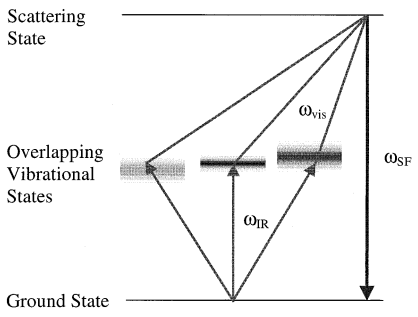

Figure 2. Energy diagram representative of a typical sum frequency transition exhibiting interference between different vibrations. In simplistic terms, the sum frequency response can be viewed as a combination of a resonant infrared transition with a nonresonant Raman transition. The overall process leaves the molecule in its original ground state. Interference patterns arise when different infrared transitions overlap, giving rise to multiple indistinguishable "paths" that give rise to the same sum frequency response. (Reprinted with permission from ref 50. Copyright 2000 American Chemical Society.)

$$\chi_{IJK,\nu} = \sum_{lmn} \boldsymbol{\mu}_{IJK:lmn} \cdot \beta_{lmn,\nu} \tag{6}$$

The indices I, J, and K represent the lab frame coordinates X, Y, or Z observed in a specific experiment. The indices l, m, and n run through the molecular coordinates a, b, and c. The orientation of the molecular axis system in the lab frame is defined by the transformation tensor, $\boldsymbol{\mu}_{IJK:lmn}$, through the Euler angles θ, φ, and χ. If the signs of $\beta_{lmn,\nu}$ and $\chi_{IJK,\nu}^{(2)}$ are known, then the average orientation of the molecules can be constrained by analyzing how the sign of the transformation tensor changes with respect to the angles θ, φ, and χ. An excellent resource for these transformation equations is given by Hirose et al.[48,49] For vapor/water and liquid/liquid interfaces discussed here, the signs of the $\chi_{IJK,\nu}^{(2)}$ terms are determined through a comprehensive fit of the observed sum frequency spectra to eqs 1 and 3, as described below in the discussion of water, and the signs of the $\beta_{lmn,\nu}$ components can be determined through ab initio calculations.[51,52]

The polarizations of the incident and outgoing fields can be used in different combinations to provide further information about the orientation of interfacial molecules. Given that the interface between two isotropic bulk media is isotropic in the plane of the interface (i.e., it has $C_{\infty v}$ symmetry), the surface susceptibility $\boldsymbol{\chi}_s^{(2)}$ which is a 27-element tensor can generally be reduced to the following four independent nonzero elements

$$\chi_{zzz}^{(2)}; \chi_{xxz}^{(2)} = \chi_{yyz}^{(2)}; \chi_{xzx}^{(2)} = \chi_{yzy}^{(2)}; \chi_{zxx}^{(2)} = \chi_{zyy}^{(2)} \quad (7)$$

where z is the direction normal to the interface. In principle, the four independent values can be determined after the acquisition of sum frequency spectra under four different polarization combinations (*SSP*, *SPS*, *PSS*, *PPP*) with the polarizations listed in order of decreasing frequency (sum frequency, visible, IR). *P*-polarized light is defined as having its electric field vector parallel to the plane of incidence, whereas *S*-polarized light is polarized perpendicular to the incident plane (see Figure 1). The *SSP* polarization combination probes modes with IR transition moment components perpendicular to the interfacial plane, *SPS* and *PSS* polarization combinations probe modes that have IR transition moment components in the plane of the interface, and the *PPP* polarization combination probes all components of the allowed vibrations.

Additional factors that must be taken into account when describing the SF response are the linear and nonlinear Fresnel factors that describe the transmission and reflection of the three light beams at the surface, with their values dependent on the optical geometry of the experiment. Fresnel factors are the reflection and transmission coefficients for electromagnetic radiation at a boundary and depend on the frequency, polarization, and incident angle of the electromagnetic waves and the indices of refraction for the media at the boundary.[47,53] The dependence of the intensities on the Fresnel coefficients under the four polarization schemes are

$$I_{PPP} \propto |\tilde{f}_z f_z f_z \chi_{zzz}^{(2)} + \tilde{f}_z f_i f_i \chi_{zii}^{(2)} + \tilde{f}_i f_z f_i \chi_{izi}^{(2)} + \tilde{f}_i f_i f_z \chi_{iiz}^{(2)}|^2$$

$$I_{SSP} \propto |\tilde{f}_i f_i f_z \chi_{iiz}^{(2)}|^2$$

$$I_{SPS} \propto |\tilde{f}_i f_z f_i \chi_{izi}^{(2)}|^2$$

$$I_{PSS} \propto |\tilde{f}_z f_i f_i \chi_{zii}^{(2)}|^2 \quad (8)$$

where the subscript i stands for x or y and f and $\tilde{f}$ are the linear and nonlinear Fresnel factors, respectively.

B. Experimental Considerations

There are numerous types of laser systems and detection methods used to conduct VSF experiments that can be found in the literature. Only general features of the experimental setup are provided here. Because of the higher order nature of the VSF response and the relatively low polarizability of most liquids, the VSF signal from aqueous surfaces is relatively weak. Hence, pulsed lasers with high peak fields are generally used. Since the sum frequency intensity increases with the peak intensity of the incident beams, picosecond and femtosecond pulses are optimal, although these shorter pulses result in larger IR bandwidths. Nanosecond systems are generally much simpler to operate and have narrower IR bandwidths but have the potential to contribute to significant heating of the interface unless care is exercised, such as employing an optical coupling scheme such as total internal reflection (TIR)[54] that can enhance the VSF signal by several orders of magnitude, or other mechanisms such as sample rotation.[55]

Most VSFS studies to date have focused on the vibrational region around 3 μm because nanosecond and picosecond systems currently generate the highest IR power densities there. Tunable IR light has been produced by a number of optical parametric generation (OPG), oscillation (OPO), and amplification (OPA) systems as well as difference frequency mixing and stimulated Raman scattering. Figure 1a shows the geometry generally used for vapor/water studies where both nanosecond and picosecond laser systems have been used. For liquid/liquid studies, the use of nanosecond lasers has been facilitated by employing a TIR geometry where the light is coupled to the interface through the organic (higher index) medium (see Figure 1b).[56,57] The incident laser beams strike the interface near their respective critical angles to generate sum frequency in reflection at its critical angle. A TIR geometry has also been used in studies of solid/aqueous interfaces where the light is passed through the backside of a transparent surface.[58,59]

Experiments employing femtosecond laser pulses have recently been reported by several groups conducting VSFS studies.[60−62] With the large bandwidth of femtosecond pulses (a few hundred wavenumbers), a significant portion of the vibrational spectrum can be obtained without tuning. McGuire et al.[60] demonstrated a Fourier transform spectroscopic technique based on VSFS. This method results in nearly unlimited spectral resolution and is based on the Fourier transform of a SF-upconverted interferogram of an IR-induced polarization on the surface of the sample. A second method[61] capitalizes on the variation of the SF exit angle as a function of SF frequency, with the SF signal collected with a multielement detector. A third method disperses the broadband SF signal generated by femtosecond IR and narrow-band visible pulses with a monochromator and records the signal with a CCD camera.[62]

Since the surface of an aqueous liquid, whether it is at a vapor/water interface or a liquid/liquid interface, provides an energetically attractive site for molecules that have both polar and apolar parts, obtaining a clean interface is a serious challenge in any VSF experiment. For example, our experiments have shown remarkable sensitivity in the VSF water spectrum to trace amounts of organic impurities that migrate to the interface.[63] If these impurities are highly surface active (this is generally the case), the spectrum of the impurity can dominate the interfacial spectrum. Therefore, samples and solvents must be highly purified, and all equipment that comes in contact with the samples must be extraordinarily clean.

III. Hydrogen Bonding and Structure of Water at Aqueous Surfaces

A. Vapor/Water Interface

The VSF spectrum of the vapor/water interface was first reported by Shen and co-workers.[64,65] In more recent years, it has been examined in additional studies as investigators have sought to unravel the complexity of the spectral response with extended experimental studies, improved analysis procedures, and advances in laser instrumentation.[50,66−69] Figure 3 shows representative spectra of the vapor/water

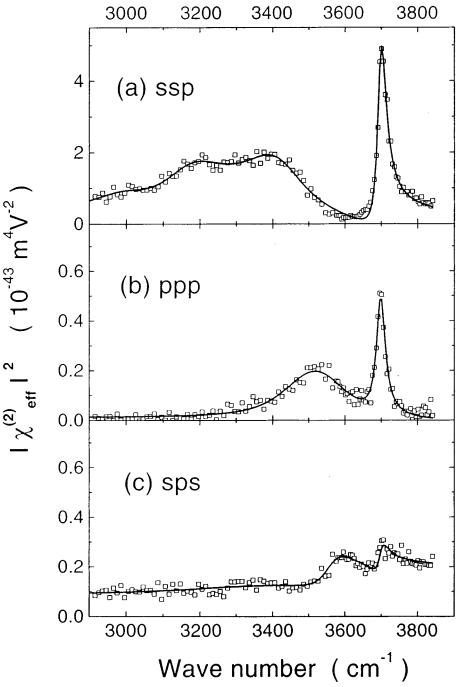

Figure 3. SFG spectra of the water surface at 20 °C with three different polarization combinations *SSP*, *PPP*, and SPS. (Reprinted with permission from ref 70. Copyright 2001 American Physical Society.)

interface recently published by Wei and Shen[70] for three different polarization combinations. With *SSP* polarization (Figure 3a), transition dipoles perpendicular to the surface plane are being sampled whereas with *SPS* (Figure 3c) transition dipoles parallel to the interface are probed. The spectral region corresponds to the OH stretching modes of surface water molecules. The vibrational spectrum of water in this region is of particular interest because the OH stretch modes are highly sensitive to the local molecular environment.[71−75] The water vibrational spectrum therefore provides a sensitive probe of the structure and energetics of the hydrogen-bond network at the interface. The sensitivity of VSFS to surface water vibrational modes is accompanied by a complexity in spectral interpretation that is only beginning to be explored by researchers in depth. This complexity is due to the variety of different environments of the interfacial water molecules and the broad nature of the peaks corresponding to water molecules that extensively hydrogen bond to other water molecules. This difficulty in interpretation is not unique to surface vibrational spectroscopy but has been a major point of controversy over the past decades in the interpretation of bulk water spectra.[71,73,74]

Assignment of spectral features in this spectrum rely heavily on IR and Raman assignments of OH stretching modes taken from bulk water measurements.[71,76−79] In most of the VSF studies, broad features in the spectrum have been assigned to vibrational modes that encompass a wide distribution of hydrogen-bonded strengths for any particular assignment.[16,43,50,64,65,67−70] The bands from approximately 3000 to 3600 cm^{-1} have been discussed in terms of symmetric stretch modes for water molecules in a broad distribution of tetrahedral bonding environments, both symmetric and asymmetric. The literature has generally discussed the broad band in this region in terms of two subbands that are centered around 3200 and 3450 cm^{-1}.[16,43,50,64,65,67−70] The former, which is comparable in frequency to the IR and Raman spectra of ice,[80] has generally been attributed to strong intermolecular in-phase hydrogen bonds of water molecules that give rise to a highly correlated hydrogen-bonding network. The spectrum represents a continuum of OH symmetric stretches (SS), ν_1 of water molecules in a symmetric environment (SS−S). For simplicity, this subband has been referred to as the "ice-like" region because of its similarity in energy to OH bonds of water molecules in bulk ice. The higher energy broad band region of ∼3250−3500 cm^{-1} is assigned to more weakly correlated hydrogen-bonded stretching modes of molecular water that encompass both ν_1 (OH symmetric stretch) and to a lesser extent ν_3 (OH asymmetric stretch) vibrational modes. Intensity in this region corresponds with OH stretch intensities of bulk liquid water and hence has been referred to as "liquidlike" hydrogen-bonding modes. These water molecules reside in a more asymmetrically (AS) bonded water environment, and hence, the intensity in this region has been labeled as SS-AS. Some differences in the spectral features in the tetrahedrally coordinated region of the spectrum are observed depending upon whether a nanosecond[69,81,82] or picosecond laser system is used,[64,66,67,70,83,84] but in general, the spectra all show similar trends. The considerable intensity in the lower subband has led Shen and co-workers[64] to conclude that the hydrogen bonding at this interface has an "ice-like" character.

A sharp spectral feature located near 3700 cm^{-1} is also observed in the vapor/H_2O spectrum. This region is characteristic of vapor-phase water molecules, and the peak corresponds to the free OH bond of surface water molecules.[64] The relatively high energy of this mode reflects its lack of donor bonding with other water molecules. This free OH bond, which is directed into the vapor phase, is energetically uncoupled from the adjacent intramolecular OH bond that does participate in H-bonding with neighboring water molecules (referred to here as the donor bond or donor mode). This situation leads to two distinct intramolecularly uncoupled OH stretching modes which, analogous to gas-phase vibrational spectra of water dimers, give rise to a free and bonded OH stretch of the H-bond donating water molecule.[85,86]

This intramolecularly uncoupled and unperturbed OH oscillator at 3700 cm^{-1} (Figure 3a) is located directly between the coupled ν_1 (3657 cm^{-1}) and ν_3 (3756 cm^{-1}) modes of monomeric vapor water, as governed by the linear superposition of states. The location of the uncoupled, bonded OH stretching mode (donor mode) has been measured recently as discussed below.[66]

Deriving a quantitative relationship between spectral intensity and the number of water molecules that have different degrees of hydrogen bonding is challenging for several reasons. First, deconvolution of the broad spectral intensity in the 3100−3500 cm^{-1} spectral region into several peaks by use of various curve-fitting routines has long been controversial for bulk water studies. The nature of the nonlinear response of VSF makes this even more complicated without employing additional experiments that can identify particular water species as has been done in other VSF studies.[63] Second, the broad spectral feature in the tetrahedrally coordinated region represents a broad range of water−water interactions and assigning peaks to specific types of interactions as one would do for more isolated water molecules is of course suspect. Third, the OH oscillator strength of a water molecule can vary significantly with the degree of hydrogen-bonding,[71,73,87] with increased bonding leading to increased oscillator strength. Thus, quantitative comparisons or even relative comparisons between intensities of OH modes that are strongly hydrogen bonded with those that are weakly hydrogen bonded require an understanding of how this bonding affects both the Raman and IR transition probabilities for each assigned mode measured by VSFS. Recall that the VSF resonant macroscopic susceptibility contains both factors (eq 3). As an alternative, an early study of the number of water molecules corresponding to the free OH mode, monitored the decrease of the free OH intensity as methanol adsorbed at the surface, as a means of quantifying the proportion of water molecules that straddle the interface. These studies suggest that at least 20% of the water molecules fall into this category.[64]

Recently there have been several studies that are providing more detailed information about interfacial water species contributing to the vapor/water interface.[50,66] The first has involved development and application of a spectral analysis procedure for fitting the VSF vapor/water spectrum that takes into account interferences that arise between nearby vibrational modes due to the different symmetries of the modes and the relative orientation of the transition dipole.[50] The second has involved isotopic dilution studies that determine the spectral contribution from the OH donor mode of the water molecules that straddle the interface.[66] Both of these studies have benefited from related studies of the CCl_4/H_2O interface (to be described later) where weaker interfacial hydrogen bonding has allowed for specific water species at this interface to be identified through complementary IR and isotopic dilution experiments.[63,88]

The most rigorous spectral analysis procedure developed and applied to the VSF spectra of water surfaces that takes into account symmetry, phase, and relative orientation has appeared in a series of recent papers.[50,63,88] Since VSFS is a coherent nonlinear spectroscopic technique, each resonant vibrational mode has an inherent phase for a fixed orientation. Resonant modes that change phase with orientation of the molecule have the capability of interfering either constructively or destructively when overlapped in frequency. The work considers a range of water species present at a water surface and the possible interference between these contributing modes and takes into account the phase of the SF response from contributing vibrational modes. This phase is useful in obtaining an average orientation of molecules at the surface by relating the macroscopic second-order susceptibility, $\boldsymbol{\chi}^{(2)}$, of the system to the molecular hyperpolarizabilities, $\boldsymbol{\beta}_{\mathbf{v}}$, of the individual molecules at the interface.[48,49] For the vapor/water spectrum, the signs of the $\chi_{IJK,\nu}^{(2)}$ terms can be determined through a comprehensive fit of the observed sum frequency spectra to eqs 1 and 3 and the signs of the $\beta_{lmn,\nu}$ components can be determined through ab initio calculations.[51,52] Application of this analysis to the weakly hydrogen-bonded region of the spectrum suggests the possible presence of weakly hydrogen-bonded water monomer-like molecules in the interfacial region. These types of water monomers were first observed in CCl_4/H_2O VSF spectrum.[63,88]

The recent isotopic dilution experiments of HOD at the vapor/water interface provide further information about contributing spectral features in the broad band between 3100 and 3500 cm^{-1}.[66] Isotopic dilution studies have been invaluable in previous studies of IR and Raman water spectra, particularly the measurement of the HOD spectrum.[41,89−93] Because of the intramolecular uncoupling of the OH and OD modes, the VSF spectrum is much simpler and allows spectral-fitting procedures to be used that measure and enable separation of the nonresonant background signal from the resonant signal. The measurement of the VSF spectrum of HOD in D_2O at the vapor/water interface provides a means of identifying the spectral region for contributing hydrogen-bonded modes such as the donor mode of the water molecules that straddle the interface and the double donor mode of water molecules with their oxygen atoms pointing out of the interfacial region.

Figure 4(a−d) shows the VSF spectra in the OH stretch region of the vapor/water interface with differing concentrations of $HOD/D_2O/H_2O$.[66] The top spectrum corresponds to the vapor/H_2O interface, analogous to that shown in Figure 3a. The difference in the relative height of the free OH band and the broad bonded OH band for these two spectra from different laboratories is due to a difference in correction for the linear-IR Fresnel coefficient. For Figure 4a the linear Fresnel coefficient used has been calculated as a function of frequency (to correct for the dispersion in the index of refraction),[66] whereas for Figure 3a a constant index of refraction has been employed.[70] The experimental data from these two laboratories prior to this correction are otherwise

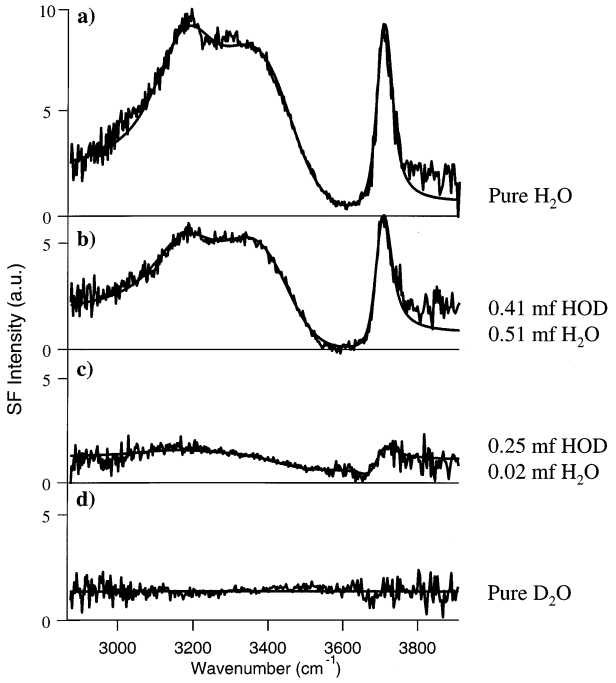

Figure 4. VSF isotopic dilution measurements of the OH stretch region for vapor/water interface with differing mole fractions (mf) of HOD, H_2O, and D_2O. Solid lines are the best fits to the resonant + nonresonant response. *SSP* polarization. (Reprinted with permission from ref 66. Copyright 2002 American Chemical Society.)

identical including the relative height of the free OH and bonded OH modes. With increased D_2O in the aqueous solution (Figure 4b−d), the number of contributing OH oscillators decreases as manifested in the decrease in the resonant contribution from the OH oscillators. The VSF response from the pure D_2O spectrum (Figure 4d) provides an important measurement of the nonresonant VSF background that is necessary to include in spectral analysis and fitting. Because of the complex nature of the VSF response, this background cannot merely be subtracted but must be deconvolved from the resonant response. This is easiest to achieve for the spectroscopically simplest system where HOD and D_2O are the dominant species at the water surface (Figure 4c). The resonant response after removal of the nonresonant background is shown as a solid line (Figure 5a). The contributing peaks (dotted lines) derived for this spectrum from the best fit to the experimental data are also shown in Figure 5a. The overall best spectral fit to the data which includes the nonresonant response and the contributing resonant peaks is shown as a solid line in Figure 4c. The HOD surface spectrum (Figure 5a) is dominated by the free OH mode at 3694 cm^{-1} and a broader peak near 3420 cm^{-1} that the authors attribute to the OH bond of HOD that is directed into the aqueous phase, the donor mode. The frequency of the donor mode is similar to that measured for the donor mode of HOD at the CCl_4/HOD/D_2O interface.[88] Also contributing in this spectral region are water molecules that on average have both their OH and OD bonds directed into the aqueous phase with the OH bond having a component perpendicular to the interfacial plane (double donors). There are also two weak broad peaks

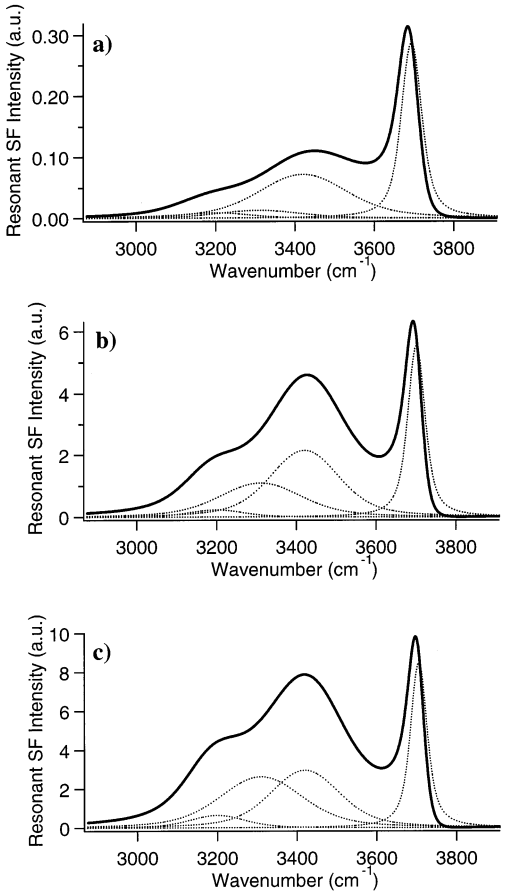

Figure 5. Resonant contributions (solid line) to the VSF spectra of Figure 4 for (a) 0.25/0.02/0.73 mf of HOD/H_2O/D_2O; (b) 0.41/0.51/0.08 mf HOD/H_2O/D_2O, and (c) 1.0 mf H_2O. Spectral peaks (dotted lines) contributing to the resonant response as determined by the described spectral fitting procedure. *SSP* polarization. (Reprinted with permission from ref 66. Copyright 2002 American Chemical Society.)

in the 3200, 3310 cm^{-1} region that the authors attribute to more strongly bonded H_2O molecules that are present in low concentrations. In addition to establishing the positions of the spectral peaks, the free OH and donor OH peaks are found to be 180° out of phase, consistent with the opposite orientation of these modes relative to the interfacial plane. A similar analysis has been applied to the other isotopic mixtures of Figures 4 and 5. The peak areas of the contributing OH oscillators scale appropriately with the number of OH oscillators at the interface as the H_2O/D_2O concentration is varied, providing further evidence for the validity of the spectral analysis.

The derived resonant spectral response for the vapor/water interface allows a refinement of the earlier picture of contributing species in the vapor/water spectrum. The solid line in Figure 5c corresponds to the resonant VSF spectrum of the vapor/H_2O interface after removal of the nonresonant component and the correction for the dispersion in the index of refraction. A large portion of the intensity in the vapor/water spectrum near 3450 cm^{-1} can be attributed to the donor mode of water molecules that on average straddle the interface and other partially hydrogen-bonded interfacial water molecules (double donor) near 3350 cm^{-1}. Intensity from

these bonds and the free OH bond contribute to a significant fraction of the overall intensity in the spectrum, not surprising since the polarization combination being used samples modes perpendicular to the interface and all of these have a considerable contribution in this direction. Also, these studies suggest less intensity in the 3200−3300 cm^{-1} region of the spectrum, less evidence for symmetrically tetrahedral coordinated water molecules than suggested in previous studies.[16,43,50,64,65,67−70] Further evidence of a more "liquid-like" surface, rather than one that has a structure more analogous to ice, comes from the frequency and bandwidth of the HOD spectrum of Figure 5a that are similar to what is obtained for HOD in D_2O at room temperature. In these studies the OH from HOD in D_2O is near the 3420 cm^{-1} measurement made in the surface VSF studies. The OH spectrum of HOD in this region is known to be highly temperature dependent and consequently a good indicator of the bonding environment of water molecules.[71,94] HOD in D_2O near 0 °C is in the region of 3250−3300 cm^{-1}.[93] One might conclude from these results that, given the fact that the transition probability of hydrogen-bonded species increases with hydrogen-bond strength, the surface is largely comprised of water molecules that on average straddle the interface or act as double donors. However, the additional factor that must be taken into account is that these spectra largely represent water molecules with nonisotropic directional character, to which VSFS is highly sensitive. For tetrahedrally coordinated water molecules, water molecules that are directionally isotropic in the surface plane, cancellation should lead to minimal intensity from these molecules. Evidence for this comes from the in-plane response measured by Wei and Shen that shows virtually no intensity in the 3200−3300 cm^{-1} region of the spectrum.[70]

A theoretical analysis of the VSF spectrum of the vapor/water interface in the OH stretch region based on ab initio molecular orbital theory and molecular dynamics simulation has been performed by Morita and Hynes.[95] The essential features of the spectra of the early work of Du et al.[84] and Shultz[68,82,96] and coworkers has been reproduced and interpreted by using an approximate modeling of the molecular vibrations and thus circumventing their explicit simulation. The free OH bond band has been found to be sensitive exclusively to the surface top monolayer structure, while the hydrogen-bonded band reflects the structure of the few top monolayers. In agreement with the above-described studies[66] and those of Brown et al.,[50] they also find that the dangling and hydrogen-bonded bands have opposite signs of imaginary susceptibility, which indicate different OH orientations at the surface. They determine that the population ratio between the OH bonds in the dangling bond frequency region and those at lower frequencies can be estimated to be as 35%:65%, respectively, but conclude that this percentage is probably closer to 21% when they remove those dangling OH bonds that point inward toward the bulk. They find that the vibrational modes below 3600 cm^{-1} have overall symmetric stretching character, whereas those above 3600 cm^{-1} have overall antisymmetric character. The transition region around 3600 cm^{-1} is attributed to an inhomogeneous mixture of symmetric and antisymmetric modes, while in the tail frequency regions, the modes appear to approach localized OH stretching character.

B. Organic/Water Interfaces

There has long been an interest in the structure of water adjacent to a hydrophobic medium. The interest arises since understanding molecular interactions of water next to a hydrocarbon or other nonpolar phase has direct relevance to areas such as micellar formation, protein folding, chemical separation, and oil extraction. There have been many theoretical efforts directed toward understanding these interfacial interactions on a molecular level,[1−15] but few experimental studies have been possible. Recently, the vibrational spectroscopy of water at an organic/water interface has been obtained.[63,88] For the studies reported, TIR VSFS has been used to measure the hydrogen bonding and orientation of interfacial water molecules at organic/water interfaces and to compare the results with the vapor/water interface. The organic liquids examined have primarily been CCl_4, hexane, and hexene. Figure 6 shows

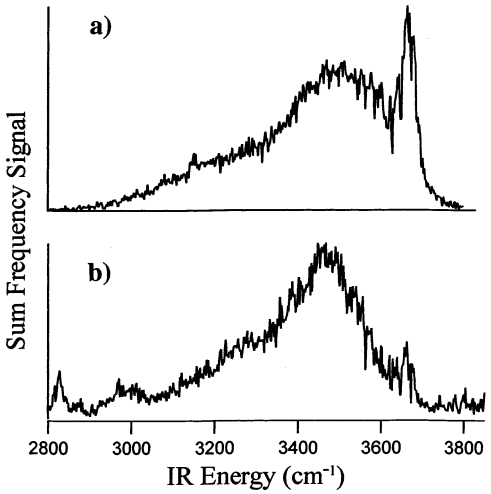

Figure 6. VSF spectrum of the (a) CCl_4/H_2O and (b) hexane/H_2O interfaces in the OH stretch region. *SSP* polarization. (Reprinted with permission from ref 63. Copyright 2001 American Association for the Advancement of Science.)

the spectra obtained from the CCl_4/H_2O (Figure 6a) and hexane/H_2O (Figure 6b) interfaces using *SSP* polarization. The spectra are dominated by intensity at higher energies (3400−3800 cm^{-1}) characteristic of weakly or non-hydrogen-bonded water molecules.[71,97,98] They both show a sharp peak at higher energies, at ∼3669 and 3680 ± 4 cm^{-1} for the CCl_4/water and hexane/water interfaces, respectively. For these TIR experiments for which a nanosecond laser system is used, the nonresonant signal as measured by D_2O experiments is negligible. Consequently, the spectra shown represent the resonant OH response. A comparison of these spectra of Figure 6 with the resonant response from the vapor/water interface (Figure 5c) indicates that the hydrogen-bonding

interactions at the liquid/liquid interface as probed by *SSP* polarization are weaker than that of the vapor/water interface, as indicated by the overall spectral intensity of the former being at higher energies than the latter. This weakening of interaction between water molecules is attributed to a reduction in the coordination number of interfacial water molecules and/or a weakening in the strength of individual hydrogen bonds between interfacial water molecules as they interact with the organic phase.

The weaker nature of the hydrogen bonding at this interface has facilitated assignment of spectral features in the CCl_4/H_2O spectrum. The "free OH" mode for water is clearly apparent at the CCl_4/H_2O interface, but its energy is red shifted (3669 ± 4 cm^{-1}) relative to the vapor/water interface (3702 cm^{-1}).[64,65,67] From studies of HOD monomers in CCl_4, the study has determined that this red shift is due to an attractive interaction between the dangling OH bond and the surrounding CCl_4 molecules.[63] The binding energy for the H_2O-CCl_4 complex is reported to be -1.4 kcal/mol.[99] The results are consistent with simulations of this interface that suggest a locally sharp transition between phases.[11,100,101] VSF studies of HOD at this interface provide further assignments. In addition to the free OH bond and free OD bond of HOD at the interface (measured at 3664 and 2712 cm^{-1}, respectively), a broader peak is observed near 3450 cm^{-1} that is attributed to the donor OH mode of the water molecules that straddle the interface or water molecules with both bonds directed into the aqueous phase (double donor). This is similar to what is observed in the follow-up studies described above for the vapor/water interface,[66] but in the CCl_4/H_2O studies, the negligible nonresonant background simplifies the analysis. The remaining portion of the H_2O spectrum of Figure 6a between 3450 and 3700 cm^{-1} is attributed to weakly interacting water molecules that are either surrounded by CCl_4 or bonded to other water molecules as electron donors only.[63] Since the true monomers and the electron donor water molecules are spectroscopically indistinguishable in these experiments, the authors refer to them as "monomer-like". The OH stretch of water monomers in bulk CCl_4 show two characteristic peaks in the IR spectra, one associated with the symmetric OH stretch (SS or ν_1) of water monomers (3616 cm^{-1}) and the other (3708 cm^{-1}) associated with the asymmetric OH stretch (AS or ν_3). These two peaks energetically bracket the dangling bond stretch mode in the VSF spectrum. Careful analysis of the data shows that both the SS and AS modes of monomer-like water molecules are present in the VSF spectrum, which respectively constructively and destructively interfere with the neighboring dangling OH bond mode.[50] The authors conclude from the fits and the derived sign of the phases that the SS and AS observed intensities represent water molecules at the interface that have a net orientation with their hydrogens pointed into the CCl_4. The peak energies and widths determined from the fits agree well with FTIR data of water monomers in bulk CCl_4. The orientation of these water molecules into the CCl_4 phase is attributed to the interfacial electrostatics which includes the nonnegligible H_2O-CCl_4 interaction. The authors demonstrate how the orientation of these monomer-like water molecules can be flipped 180° by variation of the pH in the aqueous phase.[63,88]

Overall, the results suggest that, relative to the vapor/water interface, the hydrogen bonding at the CCl_4/H_2O and hydrocarbon/H_2O interface is very weak. Intensity is observed in the strongly hydrogen-bonded region (3200−3400 cm^{-1}), but overall the spectra are dominated by water species that have only weak interactions with other water molecules and CCl_4 molecules. This is the first spectroscopic evidence for the existence of monomeric and monomer-like water molecules at a water/hydrophobic interface. Figure 7 shows the fit (top) and contributing

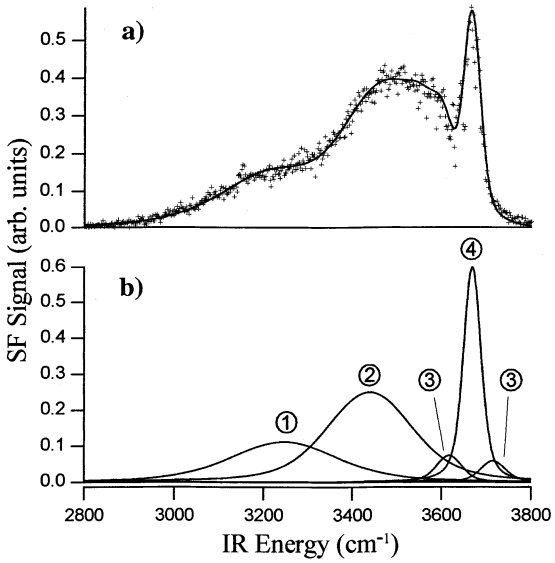

Figure 7. (a) VSF spectrum of the CCl_4/H_2O spectrum with the overall fit (upper). (b) Contributing spectral peaks for the various OH modes derived from the fit to the data in part a and shown schematically in Figure 8. Peaks labeled 1, 2, and 3 are determined from the fit to be 180° out of phase from 3 and 4. See text for details. (Reprinted with permission from ref 63. Copyright 2001 American Association for the Advancement of Science.)

spectral peaks (bottom) derived from the data described above for CCl_4/H_2O. Figure 8 provides a schematic of the different water species corresponding to the spectral peaks in Figure 7 derived from the combination of experiments and fitting. The relative phases derived from the fit to the data provide the necessary orientation of the water molecules that are depicted. For example, under *SSP* polarizations, the SS and AS of monomeric H_2O (labeled as 3) have opposite sign conventions (+ and − respectively), meaning they are near 180° out of phase.[50] Given that the OH dangling bond (+ sign convention and labeled as 4) has a significant contribution perpendicular to the interface, if the water monomers are oriented with their dipoles in the same direction as the dangling bond, the SS(+) and AS(−) modes should constructively and destructively interfere, respectively, with the dangling bond mode. This is what is observed. Spectral fits place the AS and SS of these monomer and monomer-like waters with their hy-

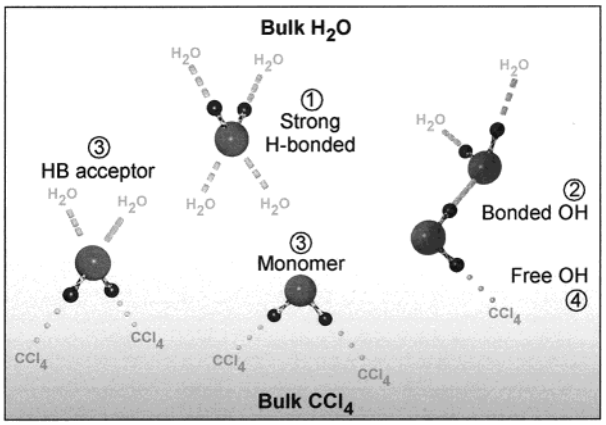

Figure 8. Schematic of the water molecules at the CCl_4/H_2O interface as determined by the VSF spectroscopy of this interface. The numbers correspond to the spectral peaks shown in Figure 7b. (Reprinted with permission from ref 63. Copyright 2001 American Association for the Advancement of Science.)

drogens oriented into the CCl_4 phase at 3616 ± 2 and 3706 ± 2 cm^{-1} respectively, compared with the FTIR measured peaks at 3616 and 3708 cm^{-1}.

These results for the CCl_4/H_2O and hexane/H_2O[63] and other alkane/water[101] systems described are distinctly different than previous related studies of the CCl_4/H_2O interface by Gragson et al.[38] and the hexane/H_2O interface by Du et al.,[64] which both exhibited little spectral intensity in the 3500−3600 cm^{-1} region and large intensities in the 3200 cm^{-1} region. This has been interpreted as an enhancement of the water structure at these surfaces. However, it has been discovered in these later studies and confirmed by surfactant addition studies that the VSF spectrum of interfacial water is *highly* sensitive to trace amounts of impurities (10−100 nM) that tend to concentrate at the interface. As the impurities are progressively removed, spectral features in the 3400−3600 cm^{-1} region grow in and spectral intensity in the 3200 cm^{-1} region diminishes resulting in the VSF spectrum in Figure 6a and b. These findings have therefore modified previous interpretations and can readily account for the differences between these observations and previous CCl_4/H_2O [102] and hexane/H_2O[65] VSF studies.

Recent molecular dynamics simulation studies of the organic/water interface have shed further light on water structure and hydrogen bonding at these interfaces as well as the interpretation of the VSF results of these systems.[101] MD simulations of the CCl_4, hexane, and vapor/water interfaces have been conducted using the AMBER suite of MD programs. The SPC/E model was used to describe all water molecule interactions. The method of Morita and Hynes[95] was used to calculate VSF spectra for these interfaces to allow for comparison with the experimental data. For the CCl_4/water interface, the free OH is calculated to be oriented on average roughly 30° from the surface normal, resulting in a strong SF response under SSP polarization. The donor OH bonds are pointing into the bulk water (110° from normal) and consequently have a smaller and oppositely signed contribution to $\chi_{SSP}^{(2)}$ than the free OH bonds. Interfacial forces also orient a large number of water molecules in the interfacial region with both hydrogens participating in hydrogen bonding with other water molecules. The interfacial molecules with this type of stronger hydrogen bonding are found, on average, to have both of their hydrogens near the plane of the interface (∼95° from normal) toward the bulk water. The interfacial depth probed by the VSF experiments can be estimated from the simulation. The simulated hexane/water interface, for example, displays a net orientation of water molecules for a total of 9 Å. The full width half-maximum of $\chi_{SSP}^{(2)}$, an alternative depth, was determined to be 4.5 Å. The VSF spectra calculated from these MD simulations for hexane/water and CCl_4/water show remarkable agreement given the three-point model used in the simulation. In both cases a sharp free OH peak is observed at ∼3700 cm^{-1} as well as a broad hydrogen-bonded feature centered at ∼3400 cm^{-1}. The calculated relative intensities of the vibrational features for these two systems also compare well with the experimental results.

C. Water at Solid Surfaces

The molecular interaction of water with solid surfaces forms the basis for a wide range of important chemical and physical processes including wetting, corrosion, friction, adhesion, and erosion. For hydrophilic surfaces, bonding interactions between the substrate and the water molecules can lead to complete wetting of a surface and the formation of two-dimensional films. For hydrophobic solid surfaces where molecular interactions between a largely nonpolar surface and water can lead to partial wetting, droplets are often formed on the surface. With surfaces of an ionic nature, water can form solubilized films that erode or dissolve the surface. Aqueous solutions in contact with metal and other reactive surfaces can lead to oxidation and reactivity of the surface that forms the basis of corrosive processes that diminish the structure and function of many materials. It is only recently that a detailed knowledge of the molecular interactions between water layers and various solid surfaces has begun to emerge. Vibrational sum frequency spectroscopy is playing a role in these advances as indicated by the overview given below.

1. Surface Melting of Ice

The melting of ice and the molecular structure of a liquidlike layer on a bulk ice surface has intrigued scientists for many decades. Considerable theoretical and experimental effort has been expended over the past decades in understanding the molecular properties of a melting water surface because of its importance in a wide range of processes including glacial flows, atmospheric aerosol processes, and frictional effects on ice surfaces. Experimentally, studies of ice surfaces pose challenges that are just beginning to be overcome with techniques such as IR reflectance,[78,94,103] X-ray diffraction,[104,105] proton backscattering,[106] ellipsometry,[107,108] and interference microscopy.[109] Recently VSFS has been applied to this issue.[110] In these studies, the surface melting of the (0001) face of hexagonal ice (I_h) has been studied in

the range of 175−300 K. The free OH mode has been used to monitor the degree of orientational disorder. Figure 9 shows the VSF spectrum of the (0001)

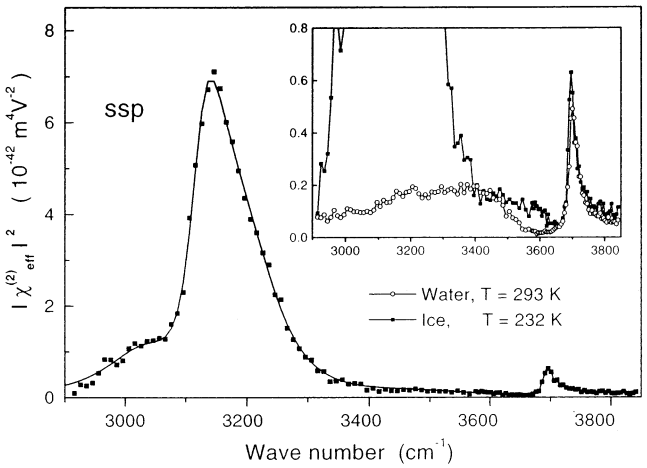

Figure 9. VSF spectrum of the (0001) surface of ice at 232 K (solid symbols). The inset shows a comparison of the spectrum with that of the water surface at 293 K (open symbols). The polarization combination is *SSP*. (Reprinted with permission from ref 110. Copyright 2001 American Physical Society.)

surface of ice at 232 K along with a spectrum of the water surface for comparison. As shown, the spectrum of ice is dominated by a strong but relatively broad peak at 3150 cm^{-1} that resembles the main O−H stretch peak observed in the Raman spectrum of I_h.[111] The strength of this mode relative to the free OH mode in the ice spectrum, particularly when compared to the liquid water spectrum, demonstrates the strong hydrogen-bonding interactions present at the I_h surface. Using polarization studies of the free OH bonds to measure the angular spread of the free OH bond orientation, an orientational parameter is derived that is used to describe the degree of ordering. The authors conclude that the onset of surface melting of ice is around 200 K, which is lower than that measured by X-ray scattering.[105] They also find that the degree of disorder of the water molecules increases with temperature. Another important conclusion drawn from the studies is that near the bulk melting temperature of 273 K, the order parameter of the ice surface is even lower than that of the supercooled water surface, suggesting that the quasi-liquid layer on ice is different from the normal surface layer of water.

2. Water Adsorbed at Solid Substrate Surfaces

The first studies of water on a solid substrate were performed at a quartz/water interface.[83] As with previous studies discussed in this review, the spectral region corresponds to OH stretch modes of water. The clean quartz surface is generally terminated by silanol groups (SiOH) that can hydrogen bond with surface water. This is certainly the case found for quartz/water studied near neutral pH as indicated by no intensity in the free OH bond region due to the bonding of water to this surface feature. The dominance of a broad peak near 3200 cm^{-1} suggests that the hydrogen bonding at this surface is highly coordinated and almost "ice-like" in nature. This and similar studies have shown that there is a strong pH dependence in the response of the OH stretch modes of water.[16,83] At both low and high pH, strong hydrogen bonding is observed as evidenced by a dominance of the OH−SS−S peak. There is a strong orientation of surface water molecules due to the effect of increased hydrogen bonding or surface field established by the different electrostatics created by the ions in solution. At intermediate pH, more bonding disorder is apparent in the spectrum. Measurements of the phase of the VSF response show that the water dipoles have flipped by 180° as the pH is adjusted from 1.5 to 12.3.[16]

Later studies by Shen and co-workers[16] examined the quartz/ice interface at various temperatures. Figure 10 shows these results. In these studies

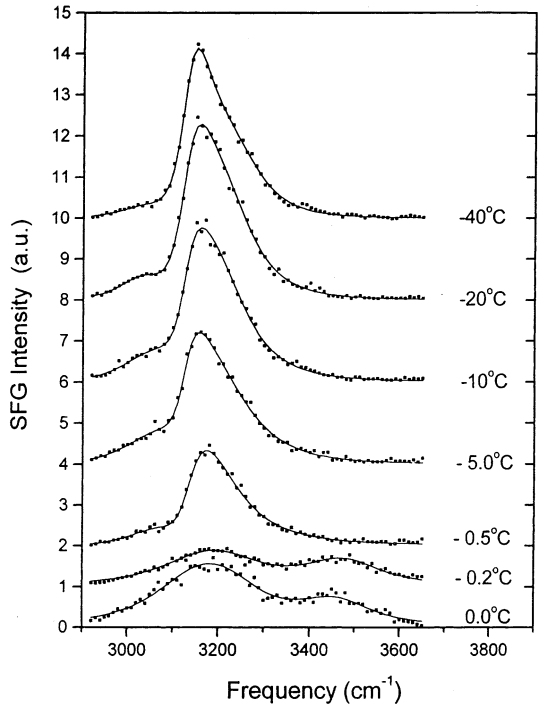

Figure 10. VSF spectrum (*SSP*) from a quartz/ice interface at various temperatures. (Reprinted with permission from ref 16. Copyright 1998 Elsevier Science.)

conducted from −40 to 0.0 °C the intensity in the OH stretch region (3600−3100 cm^{-1}) shows a shift around −0.5 °C to lower frequencies. A strong peak around 3150 cm^{-1} dominates the spectrum. The spectrum looks very similar to the ice/water spectrum described above. There is no evidence for the quasi-liquid layer at the quartz/ice interface at least up to −0.5 °C. The authors speculate the decrease in intensity with temperatures near 0 °C could be due to deprotonation of the quartz surface such that it effectively increases the number of surface defects that would disrupt the polar ordering.

Water adsorbed on a mica surface at room temperature is also found to have a more ordered hydrogen-bonding structure than bulk water.[112] These studies involved a combination of VSFS and scanning polarization force microscopy (SPFM).[113] The OD stretch modes of D_2O on mica have been explored in these studies to avoid complications arising from

the OH stretch modes that originate from the mica. The authors find that as the concentration of water on the surface increases in the submonolayer regime, the water evolves into a more ordered hydrogen-bonded network as indicated by a downshift in the OD stretch modes. At full monolayer, the VSF spectrum is indicative of an ice-like film. No dangling OD bonds are found at the mica/water interface.

The combination of VSF and thermal desorption has been used to monitor ice films grown on Pt(111).[114] In these studies the experimental results suggest that ice films grown on Pt(111) at temperatures between 120 and 137 K are ferroelectric, where "ferroelectricity" is used here loosely to describe the existence of a net polar ordering of water molecules in ice films. They observe a strong enhancement in the OH stretch resonances with film thickness that they attribute to polar ordering. Figure 11 shows the VSF results that they obtain in

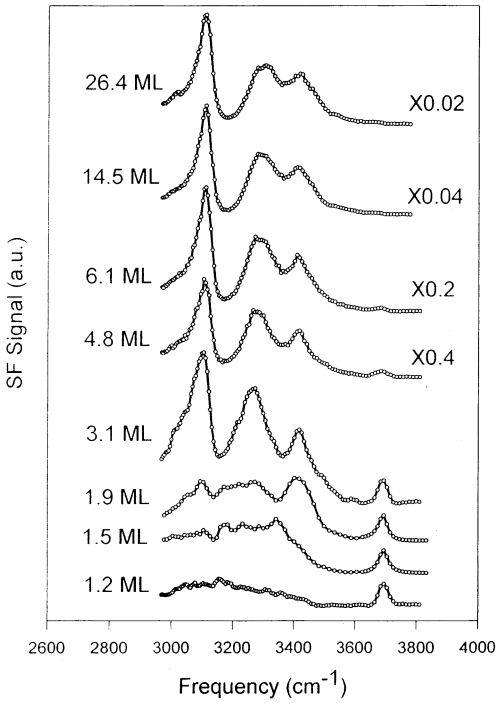

Figure 11. VSF spectra in the OH stretch region for a set of ice films of different thicknesses on Pt(111). (Reprinted with permission from ref 114. Copyright 1999 American Physical Society.)

the OH stretch region as the films grow on the surface. All incident beams and outgoing beams were *P* polarized. They attribute the increased ordering of water with film thickness to the polar anchoring of the first ice monolayer on the platinum. This surface-induced ordering is estimated to have a decay length of ~30 monolayers.

Yeganeh and co-workers[115] examined the isoelectric point of the Al_2O_3/water interface by VSFS. The isoelectric point (IEPS) of a solid surface as examined in this paper is the point at which the interfacial charge changes sign as the pH of the aqueous phase is varied. This crossing point affects many interfacial processes because as water dipoles orient differently for differing surface charges, competitive adsorption

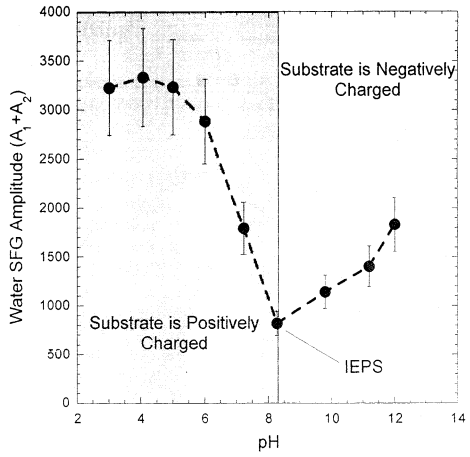

Figure 12. Variation in total water VSF signal with pH of the solution. The marked minimum in the signal strengths indicates that the IEPS of the sapphire surface is ~8. (Reprinted with permission from ref 115. Copyright 2001 American Physical Society.)

can vary on either side of this point, and the distribution of ions in the solution phase changes. Figure 12 shows the results of their studies on Al_2O_3 where the total water VSF signal is plotted as a function of the pH of the solution. The signal is found to rise on either side of the IEPS. The data were taken with *P*-polarized input and *P*-polarized VSF light detected. They show that as the pH of the aqueous phase is varied across the isoelectric point, the water dipoles flip by 180°. They also find that the signal intensity depends strongly on the hydroxyl number density at the surface. A new methodology based on surface charge density or the determination of the IEPS of a nonconductive, low surface area material is also presented.

Ionic surfaces in contact with water are challenging because of the more dynamic nature and reactive nature of these interfaces. Fluorite (CaF_2) surfaces in contact with varied aqueous solutions have been studied by Becraft and Richmond.[58] Fluorite is the primary mineral used in the production of hydrofluoric acid. Its acid/base behavior influences the adsorption of complexing agents and surfactants used to separate CaF_2 from other minerals often associated with it in the natural state. In these experiments it is shown,[58] as with quartz/water and sapphire/water interfaces, that the bonding of water molecules in the interfacial region is strongly dependent on pH. Under acidic conditions, a highly structured water phase is observed at the surface as evidenced for the strong signal near 3160 cm^{-1} (Figure 13a). As the pH is raised from 2.9 to 5.1, the VSF response in this region is found to decrease with almost a zero response at neutral pH (Figure 13a−c). The authors attribute this to the zero point of charge for this surface near neutral pH which leads to minimal water alignment. As the pH is increased, the strong hydrogen-bonding network returns but with an additional feature growing in at 3657 cm^{-1} (Figure 13f). At pH 13.7, this feature dominates the spectrum. With the aid of fluoride addition studies, the authors attribute this to calcium hydroxide species at the surface.

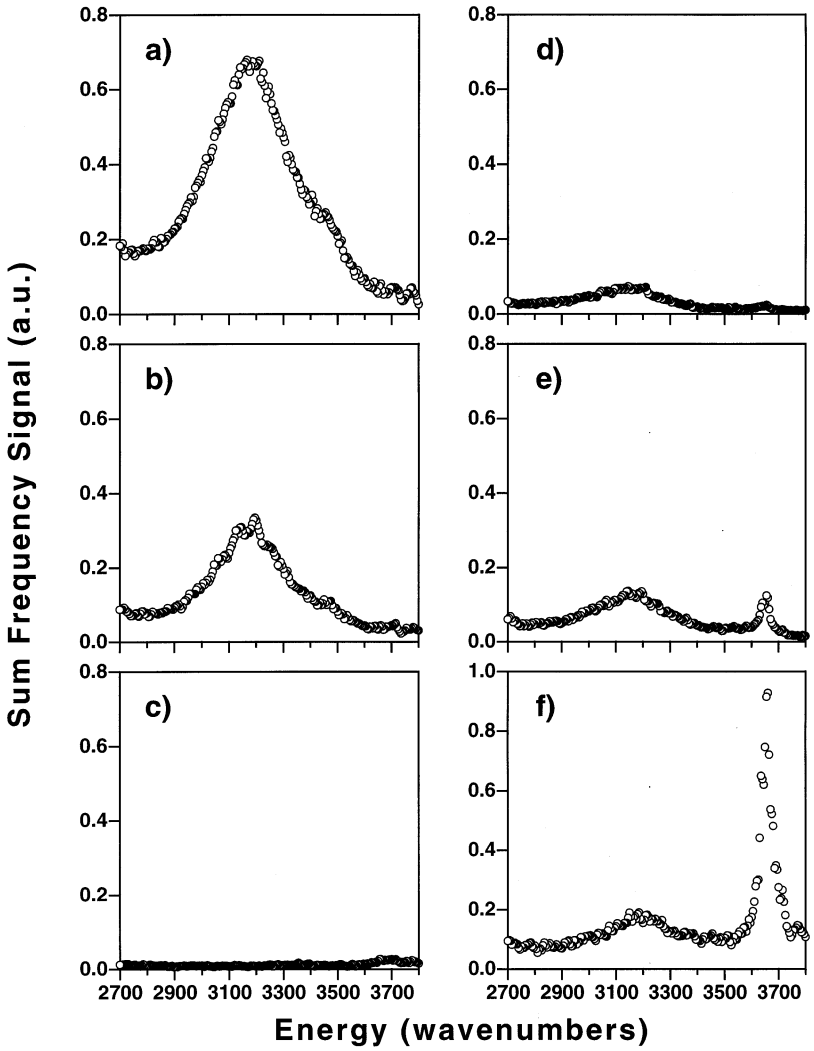

Figure 13. VSF spectrum of the CaF_2/H_2O interface at pH (a) 2.9, (b) 5.1, (c) 6.4, (d) 9.3, (e) 12.3, and (f) 13.7. *SSP* polarization. (Reprinted with permission from ref 58. Copyright 2001 American Chemical Society.)

D. Effect of Adsorbates and Ions on Surface Water Structure and Bonding

1. Alkyl Surfactants Adsorbed at the Vapor/Water Interface

When surfactants adsorb at a water surface, the surface properties are significantly altered. In particular, the lowered surface tension accompanying surfactant adsorption is one of the main reasons for the effectiveness of many surfactants in commercial products including soaps, lubricants, and detergents. The pertinent question that has been asked for several decades is how the presence of the surfactant alters the hydrogen bonding of water at these surfaces. This section reviews studies of surfactant/water interfaces that focus on the water structure. In a later section, the VSF studies that examine the structure and conformation of surfactants adsorbed at aqueous surfaces will be summarized.

A number of VSF studies have been conducted to address this particular question of what the water structure of an aqueous surface looks like in the presence of varying quantities of surfactants. These have been conducted at both the vapor/water[39,43,116,117] and the organic/water interface.[40,42,118] Most of these studies have involved examining how the OH stretching region of water (as discussed in the previous section) is altered by the presence of alkyl surfactants. In many cases deuterated surfactants are used to minimize the overlap between the OH vibrational modes of water and the C−H stretching modes of the surfactants. With these studies, a coherent picture is emerging on how the hydrogen bonding of water is affected by the presence of a surfactant at the surface. Some of the surfactants used in these studies include pentadecanoic acid (PDA) which is not charged at neutral pH and charged surfactants such as dodecyl trimethylammonium chloride (DTAC), sodium dodecyl sulfate (SDS), or dodecylammonium chloride (DAC). Earlier studies in this area have focused on surface concentrations from approximately 10^{-3} monolayer coverages to a complete monolayer coverage as indicated by a maximum in the adsorption isotherm derived from surface tension measurements.[39,40,42,43,117,118] Later studies conducted at the organic/water interface have focused on trace concentrations of surfactants at the interface (described in the next section) where headgroup areas are a more appropriate unit for the interfacial concentration.[119] In these studies, the surfactants are under

isolated conditions with headgroup areas of $>10^3$ Å^2/surfactant.

The first studies to examine both the issue of surfactant conformation and water structure simultaneously for surfactants at the vapor/water interface were conducted by Gragson et al.[43] Later studies showed a similar behavior for water at the surfactant/organic/water interface.[42] Figures 14 and 15 provide

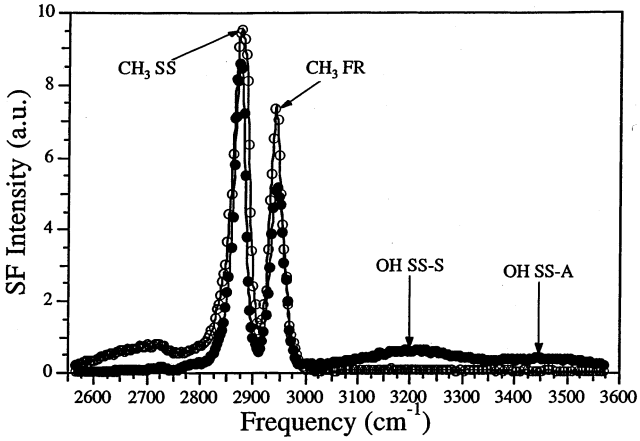

Figure 14. VSF spectra under *SSP* polarization conditions from the air/H_2O (filled circles) and air/D_2O (open circles) interfaces with a monolayer (~25 Å^2/molecules) of PDA. (Reprinted with permission from ref 39. Copyright 1996 American Chemical Society.)

a comparison of the VSF spectrum of surfactants pentadecanoic acid (PDA), dodecylammonium chloride (DAC), and sodium dodecyl sulfate (SDS) adsorbed at the vapor/water interface at approximately monolayer coverages.[39,43] For simplicity, the broad peak representing tetrahedrally coordinated water molecules is separated into two peaks, one corresponding to the OH stretch modes of symmetrically bonded water molecules (OH SS−S) and at higher energies the OH stretch of asymmetrically bonded water molecules (OH SS−A). The CH stretch modes of the surfactants correspond primarily to the methylene symmetric and asymmetric stretches (SS and AS), the methyl symmetric stretch, and a methyl Fermi resonance (FR). These modes will be discussed in more detail in section IV of this review. Both H_2O (solid circles) and D_2O (open circles) have been used as the aqueous phase to allow separation of the CH modes of the surfactant and OH modes of interfacial water. Upon comparison of the uncharged PDA (Figure 14) and the charged surfactants DAC and SDS (Figure 15), it is immediately clear that there is a large enhancement in the OH peaks of H_2O in the 3100−3500 cm^{-1} spectral region in the presence of a charged surfactant. The uncharged surfactant (PDA) at the surface causes minimal change in the OH stretching region relative to a neat water spectrum. When equal concentrations of mixed surfactants (DAC and SDS) adsorb at the interface, the surface water spectrum also shows minimal change.[43] The authors attribute the observed enhancement in the OH stretch modes at lower energy in the presence of charged surfactants to an increased alignment of the interfacial water dipoles induced by the large electrostatic field present at these charged

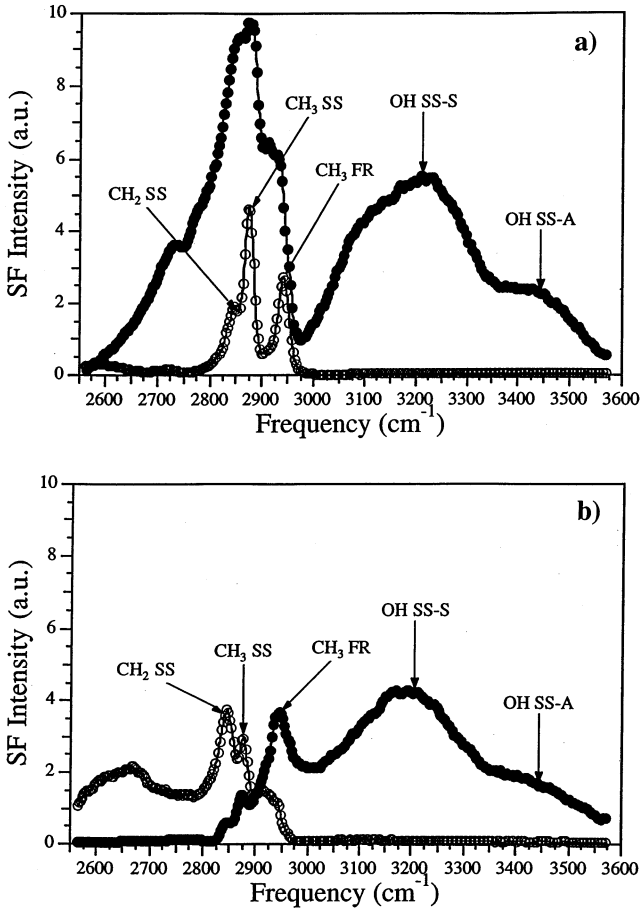

Figure 15. VSF spectra under *SSP* polarization conditions from the air/H_2O (filled circles) and air/D_2O (open circles) interfaces with (a) 14 mM DAC solution and (b) 8.1 mM SDS solution. (Reprinted with permission from ref 39. Copyright 1996 American Chemical Society.)

interfaces. The interfacial water molecules are found to attain their highest degree of alignment in the double layer region at surface surfactant concentrations well below maximum surface coverage. A second factor is the increased number of water molecules being sampled due to the effect of the double layer field established at the surface. As discussed in section II, the field effect leads to an additional contribution to the VSFS response at the interface, a third-order polarization term $P^{(3)}$, which contains the electrostatic field dependence of the nonlinear polarization induced at the interface. This field-induced third-order polarization has been examined in previous SHG studies.[120−122] In the absence of a large electrostatic field, one would expect the interfacial water molecules to be randomly oriented beyond the top few water layers and thus not to contribute to the VSF response. However, the presence of a large electrostatic field aligns the interfacial water molecules beyond the first few water layers and thus removes the centrosymmetry over this region, allowing more water molecules to contribute to the nonlinear polarization.[39,43] Ionic strength studies provide further confirmation for these conclusions. These studies show a decrease in enhancement of OH SS modes with increased ionic strength. As the ionic strength is increased, there is an increased screening of the surface charge or, alternatively, a change in

the Debye−Huckel screening length, consistent with the observations. Similar observations of enhanced OH signal were made in pH-dependent studies of fatty acid hexacosanoic acid studied at the vapor/water interface as a function of pH.[117,123] As the fatty acid becomes ionized at higher pH values, the signal in the OH stretching region increases.

Another important observation apparent in Figure 15 is the interference observed between OH stretch and CH stretch modes of the water and surfactant, respectively.[43] The DAC spectrum shows destructive interference near 2970 cm^{-1} between the OH−SS−S mode and the CH_3−FR mode (Figure 15a). The SDS spectrum shows a constructive interference between these two modes (Figure 15b). The authors attribute this difference in the interference for cationic and anionic surfactants to differing orientations of the interfacial water molecules, which results from opposite electrostatic fields created by surfactants of opposing charge. From this they conclude that the orientation of interfacial water molecules in the presence of adsorbed cationic surfactants is with the oxygen atom pointed toward the air and for the anionic surfactant with the oxygen atom pointed toward the bulk solution.

The two contributing factors to the increased OH intensity in the presence of surfactant, the increased sampling volume due to the change in Debye−Huckel screening length and field-induced orientation of water molecules, have been studied extensively in work with ionic strength studies and deuterated surfactant studies.[42] The interfacial potential was varied by changing the surface charge density (surfactant concentration), the ionic strength, and the temperature while monitoring the OH stretching modes of water. As the potential is increased at the vapor/water interface, there is a progression toward more tightly bound interfacial water molecules as manifested in an increase in intensity in the OH−SS−S stretch region relative to the SS-AS region. The authors conclude that this progression is a direct consequence of the induced alignment of the interfacial water molecules resulting from the large electrostatic field produced in the interfacial region due to the charged surfactant. Temperature-dependence measurements support this conclusion.

2. Alkyl Surfactants Adsorbed at Organic/Water Interfaces

The effect of surfactant on the ordering of water at the organic/water is important in understanding the role of water in the structure and formation of microstructures such as micelles, vesicles, and other three-dimensional structures. These all involve a charged interface between water and a hydrophobic medium such as the interior of a micelle or vesicle. There are a number of studies that have examined the effect of surfactant adsorption on the hydrogen bonding between water molecules at the organic/water interface. These studies, which have been exclusively conducted in this laboratory at the CCl_4/water interface, can be divided into two concentration regimes. The earlier studies have focused on interfacial concentrations in the 10^{-3} to 1 monolayer range.[41,42] The second, more recent, set of experiments has been conducted at trace interfacial concentrations.[119] The higher concentration experiments involved the types of measurements described above for the vapor/water interface where the interfacial potential was varied and the water hydrogen bonding examined.[42] In these studies conducted at the CCl_4/water interface, similar trends are observed as in the vapor/water studies in that an increased concentration of surfactant results in a strong growth in OH stretch contribution corresponding to tetrahedrally coordinated water molecules. The spectra of a monolayer of SDS at the vapor/water and CCl_4/water interfaces are remarkably similar, (Figures 15b and Figure 16). Both spectra show strong intensity in the OH−SS−S region of the spectrum, indicative of strong hydrogen bonding interactions. Isotopic dilution studies of this interface in the presence of a monolayer of surfactant have also been conducted.[42] These studies show a progressive shift in the OH stretching region to the blue as H_2O molecules are replaced by HOD molecules in the interfacial spectrum. The frequency of the bonded OH bond of HOD in the presence of the surfactants is found to be centered at 3460 cm^{-1}.

The more recent studies of the effect of adsorbed surfactant on the water hydrogen-bonding structure have been conducted over a broader concentration range from trace interfacial concentrations to fractional monolayer coverage, with the majority of the focus of these studies on the low concentration regime.[119] As mentioned in section III.B, the VSF spectrum of interfacial water at the organic/water interface is highly sensitive to trace amounts of charge at the interface. This observation has led to a series of studies that examine how the water structure at the organic/water interface changes as the surfactant aqueous-phase concentration is varied from nanomolar aqueous-phase concentrations, where the interfacial concentration is so low that the system can be viewed as composed of isolated surfactants, to micromolar concentrations where electrostatic interactions between surfactants and their solvating interfacial water molecules occur and interfacial potentials become more homogeneous across the interface. Figure 16 provides a view of the large changes that occur in the VSF spectrum at an organic/water interface as the SDS interfacial concentration is varied over a wide concentration range. As the concentration is increased toward monolayer coverage (5 mM), spectra similar to the earlier CCl_4/water studies[42] and the vapor/water studies described above are progressively observed.[43] The intensity in the tetrahedral bonding region grows in and eventually dominates the 5 mM spectrum with the accompanying appearance of the CH modes of the surfactant. As discussed in detail in the vapor/water studies, this growth in intensity from the OH modes of water in the 3100−3300 cm^{-1} region of the spectrum at these coverages is due to a combination of an increased contribution from strongly hydrogen-bonding water species, an increased probe depth due to the electrostatic field at the interface (an additional $P^{(3)}$ effect), and an increased orientation of interfacial water molecules induced by this field. Also observed

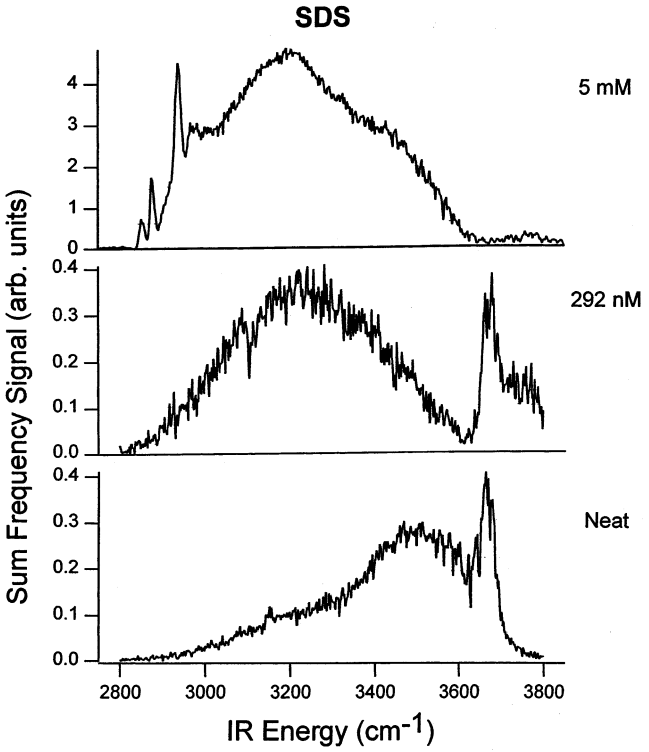

Figure 16. VSF spectra of the CCl_4/H_2O interface over a range of bulk concentrations of SDS. *SSP* polarization. The highest concentration corresponds to approximately a monolayer of SDS at the interface.

is a progressive loss in free OH intensity with higher surfactant concentration, indicative of a surface that is increasingly covered by surfactant which bonds to the free OH. Unlike the previous CCl_4/H_2O studies of water,[42] these were conducted with a nanosecond laser system (TIR geometry) with IR tunability in the free OH region.

3. Solutes, Acids, and Salts in the Aqueous Phase

There have been a number of VSF studies of the vapor/water interface that have focused on how the surface water spectrum changes with acidity and ionic concentration. These studies are relevant to understanding atmospheric reactions where aerosols can have very high concentrations of acids and high ionic strength. Some of the first and most comprehensive studies in this area have examined the structure of surface water for solutions of sulfuric acid and related salts.[68,69,124−127] Figure 17 provides an example of how the VSF spectrum of water changes for different concentrations of aqueous solutions of sulfuric acid.[123,124] The overall trends in the spectra have been seen in the other studies of this system by Schultz and co-workers.[69,125−127] As shown in Figure 17, at low concentrations of acid, the intensity at lower frequencies below 3400 cm^{-1} is found to increase. Both sets of studies conclude that there is significant orientation of surface water molecules at lower acid concentrations. Second, with increased acid concentration, the free OH mode decreases and eventually disappears. At the highest concentrations, the OH spectra decrease and eventually disappear. Raduge et al.[124] observe a low-frequency shoulder at ~3060 cm^{-1} that they assign to the acid OH stretch vibration, suggesting that the acid concentration is appreciable. This peak is not observed in the studies of Baldelli et al.[126,127] Beyond this point there is also considerable disagreement with regard to the interpretation of the data. Baldelli et al.[126,127] attribute the increased intensity at lower frequencies in the low acid region to an electric double layer at the interface, as negative ions preferentially adsorb at the liquid surface, and the drop-off in intensity at higher concentrations to disordering of the surface water. At higher concentrations, Raduge et al.[124] conclude that the surface takes on a more crystalline structure, resembling that of a crystalline sulfuric acid hydrate with the molecules arranged in a centrosymmetric layered structure with the hydrogen bonds in the surface plane leading to vibrational modes that are SF inactive. Studies of supercooled sulfuric acid solutions by Schnitzer et al.[69] indicate that the water surface of liquid sulfuric acid solutions does not vary with temperature.

Several other acid and salt solutions have also been studied by Schultz and co-workers.[68,128,129] The structure of water on HCl solutions has been examined by VSF with the primary conclusions being that ions in solution cause water on the surface to be reoriented relative to pure water with the hydrogen atoms directed toward the bulk solution. No signal due to molecular HCl was observed, suggesting to the authors that oriented water molecules and not molecular HCl dominate the surface.[128] For HNO_3 solutions and liquid HNO_3,[129] the VSF studies indicate that the surface consists of an electric field double layer comprised of subsurface anions and cations at low mole fractions (0.005 and 0.01 mole fraction of HNO_3). These solutions are found to show more VSF signal from OH stretch modes in the hydrogen-bonded region than simple salt solutions (NaCl, $NaNO_3$, $KHSO_4$), which the authors attribute to the subsurface electric field that aligns water molecules along the surface normal. At higher concentrations where the intensity is reduced, the authors conclude that ionic complexes or molecules approach the surface and disrupt the hydrogen-bonding network at the water surface.

IV. Adsorbate Structure and Bonding at Aqueous Surfaces

A. Surfactants at Vapor/Water Interfaces

Whereas many of the above-described studies have focused on the effect of adsorbates on the interfacial water structure, in the following sections the molecular structure of the adsorbed species has been probed. The most extensive studies to date have been on surfactant structure where the surfactants consist of a polar or ionizable headgroup and a nonpolar hydrocarbon chain. Such molecules readily migrate to the interface where their long alkyl chains extend into the hydrophobic portion of the interface (i.e., the air or organic phase) and the polar headgroup prefers the more aqueous portion of the interfacial region. A

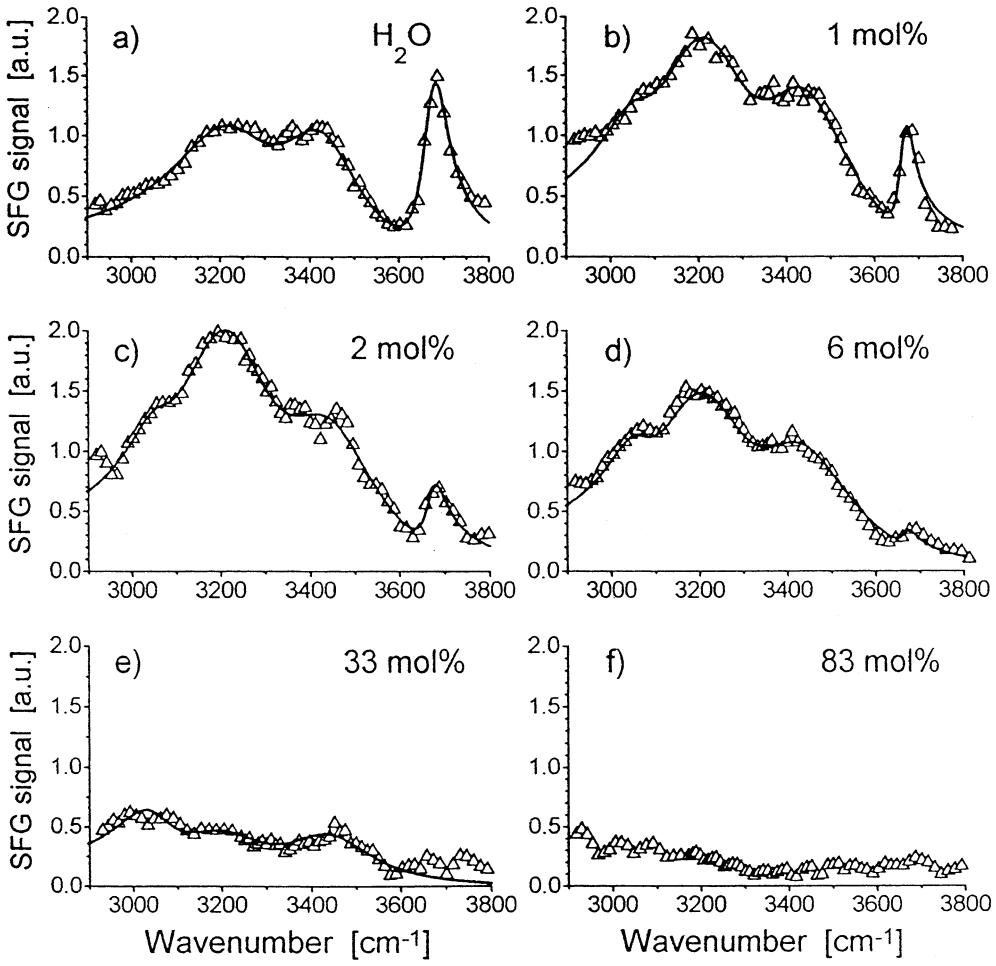

Figure 17. VSF spectra of pure water and sulfuric acid−water mixtures (with different acid concentrations as indicated) at the liquid−vapor interface at 20 °C. *SSP* polarizations. (Reprinted with permission from ref 124. Copyright 1997 Elsevier Science.)

wide variety of surfactants of this nature have been studied, with the majority of the studies focused on measuring the conformation of the alkyl chain as a function of surface concentration, surface pressure, and aqueous-phase composition.

The first studies to demonstrate that VSFS could be used to measure the molecular conformation of surfactants adsorbed at an vapor/water surface involved PDA. In these and follow-up studies, the CH stretch modes of the alkyl chain were monitored with various polarization combinations as the surface concentration has been varied in a Langmuir trough from the liquid-condensed (LC) to liquid-extended (LE) phase.[130,131] In the spectra presented as well as in later studies of PDA, the CH spectral region of this insoluble monolayer consists mainly of CH modes of the terminal methyl group.[39] Figure 14a shows an example of a spectrum of PDA at the vapor/water interface using *SSP* polarization which is similar to what has been obtained in the earlier work.[130,131] This figure however also includes the OH stretch modes of surface water for reference to the earlier discussion in this review of how the surface water spectrum is altered by the presence of a surfactant. As shown, two vibrational modes dominate the spectrum of adsorbed PDA, the methyl symmetric stretch mode near 2875 cm^{-1} and the methyl Fermi resonance mode near 2935 cm^{-1}. At a monolayer of coverage, no contribution is seen from the methylene modes of the alkyl chain similar to what has been observed in other insoluble surfactant systems.[39,54] For amphiphilic molecules that form well-ordered monolayers, in a predominantly trans conformation, the CH_2 bonds have their dipoles directed toward opposing sides of the carbon backbone. This orientation produces a cancellation of the CH_2 stretching vibrational modes, and thus, a monolayer with no or few gauche defects will exhibit only CH_3 vibrational modes in the SF spectrum. In the earlier work of Shen,[131] these CH_2 modes near 2850 cm^{-1} and in the 2930−2880 cm^{-1} region begin to appear as the surface pressure of the monolayer changed. They concluded that these observations confirm the existence of highly ordered alkyl chains with nearly normal orientation when the monolayer is in the liquid-crystal (LC) phase. In the liquid-expanded (LE) phase, the chains were found to have significant gauche defects as seen by the appearance of CH_2 modes.

A number of studies of different alcohols adsorbed at the vapor/water interface have been conducted. For the simplest alcohol, methanol, information about the molecular orientation of methanol at the water surface has been obtained by monitoring the CH stretch modes under different polarization combinations.[132] The authors find that there is an excess number density of methanol at the interface as

compared to the bulk concentration in agreement with surface tension measurements. They find that in a narrow range of bulk concentrations of methanol, the SF spectrum of the surface molecules changes drastically. They attribute this to a special structure of $CH_3OH:H_2O$ surface network. Another study examined the VSF spectra of the liquid−vapor interface for n-alcohols of (C_1−C_8).[133] In these experiments, all alcohols studied were found to be polar oriented with the alkyl chains pointing away from the liquid. For the longer chains of hexanol, heptanol, and octanol, significant contributions from CH methylene modes suggest the presence of gauche defects in the alkyl chains. In the water OH stretch region, the shift in spectra to lower frequencies indicates a well-ordered hydrogen-bonding network at the interface.[133] More detailed studies of medium chain alcohols of C_9−C_{14} have been conducted with VSF and ellipsometry by Bain and co-workers.[134,135] These studies determined that gauche defects are evident in the solid monolayer phase and increase only slightly in the monolayer just above the phase transition. Using a model of the chains as rigid rods, they calculated the area per molecule and the chain tilt in the liquid phase from the VSF and ellipsometry data. They find that the area per molecule and tilt angle increase monotonically with chain length. The density of the hydrocarbon chains in the liquid monolayer phase is found to be less dense than that in the solid monolayer phase but significantly higher than in the bulk liquid alkane. Additionally, the area per molecule, chain tilt, and volume per methylene group in the liquid phase all increase with increasing chain length. Studies of the absolute orientation of crystalline monolayers of amphiphilic α-hydroxy ω-bromo alcohols ($BrC_nH_{2n}OH$, $n = 21,22$) and the alkyl hydroxy esters ($C_mH_{2m+1}COO(CH_2)_nOH$, $m = 14,15$, $n = 10$) at the vapor/water interface have been reported using grazing incidence X-ray diffraction (GIXD) for the former and VSFS for the latter.[136] Crystalline monolayers of related alcohols are very efficient ice nucleators of supercooled water drops because of the lattice match between the unit cell of the crystalline monolayer cell and the *ab* lattice of hexagonal ice. The studies show the absolute orientation of the alcohol C−OH bonds at the water surface, which in turn can be correlated with the ice-nucleating behavior of the monolayers on supercooled water. Glycerol/water mixtures have been studied to learn how the glycerol and water structure changes as the composition is varied. In these studies, glycerol is found to partition to the surface at all concentrations with the surface orientation of glycerol found to be constant through most of the concentration range.[96]

The most detailed spectroscopic study and spectral analysis of alcohols has been conducted by Wolfrum and Laubereau.[46] In this study of hexadecanol at the vapor/water interface, three vibrations of the terminal methyl group have been studied. Figure 18 shows the spectrum obtained for this molecule under three different polarizations. For *SSP* polarizations (Figure 18a), the spectrum is dominated by the symmetric CH_3 stretching vibration at 2875 cm^{-1}. The maximum at 2936 cm^{-1} is attributed to an overtone of the

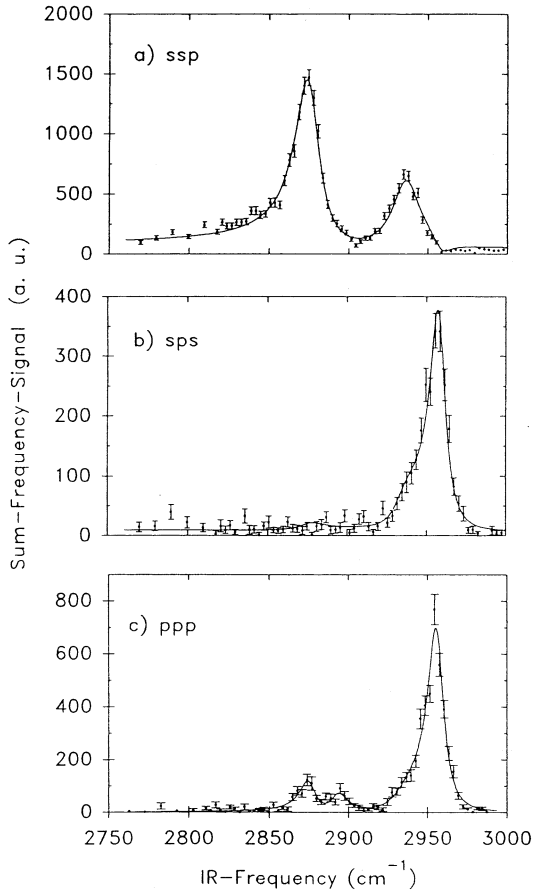

Figure 18. Measured sum frequency signal of the adsorbed monolayer of hexadecanol on water in the CH stretching region versus frequency setting of the input infrared pulse for (a) *SSP*, (b) *SPS*, and (c) *PPP* polarization combinations. The solid lines are calculated curves proportional to $|\chi^{(2)}_{yzy}|^2$*(SSP)*, to $|\chi^{(2)}_{yzy}|^2$ *(SPS)*, and a superposition of all independent components of to $|\chi^{(2)}_{ijk}|^2$ *(PPP)*. (Reprinted with permission from ref 46. Copyright 1994 Elsevier Science.)

methyl bending vibration which gains intensity by Fermi resonance with the symmetric stretching vibration. A minimum in the spectrum is observed at 2958 cm^{-1} where the degenerate CH_3 stretching vibration is expected. Neither the symmetric nor antisymmetric CH_2 stretching vibration at 2850 or 2939 cm^{-1} appear in the spectrum, indicating a straightened molecular chain in an all-trans configuration. A theoretical analysis is presented that predicts opposite phases of adjacent vibrational modes leading to destructive interference in the SF spectrum. This interference effect, similar to what was discussed above for the OH modes of water, allows the determination of the line amplitudes of the degenerate stretching mode. Figure 19 provides an example of the calculated curves used to fit the VSF *SSP* spectrum of Figure 18a and 19a and the individual contributions of the three modes to the imaginary part (Figure 19b) and real part (Figure 19c) of the contributing tensors. The relative phases of the contributions lead to the destructive and constructive interferences that contribute to the observed line shapes of the spectral peaks in the VSF spectrum. It is found, for example, that the stretching vibration and the symmetric overtone of the bending vibration

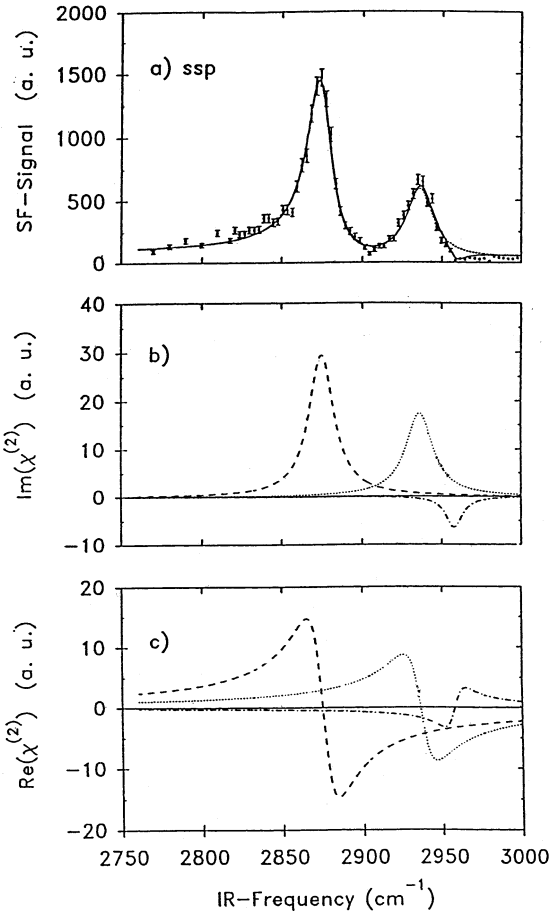

Figure 19. Measured sum frequency signal for *SSP* polarization with least-squares fit proportional to to $|\chi^{(2)}_{yyz}|^2$ as in Figure 22a. The dashed line in part a is calculated for positive amplitudes A_{yyz}, (b) imaginary part to $\chi^{(2)}_{yyz,v}$ and (c) real part to $\chi^{(2)}_{yyz,v}$ for the individual vibrational modes; (- - -) symmetric stretching vibration at 2875 cm-^{1}, (...) symmetric overtone at 2936 cm^{-1} enhanced by Fermi resonance (-·-·-) degenerate stretching vibration at 2958 cm^{-1}. (Reprinted with permission from ref 46. Copyright 1994 Elsevier Science.)

have the same phase, whereas the contribution of the degenerate vibration has the opposite phase. Destructive interference can occur in the high-frequency wing of the overtone, leading to the distinct minimum at 2958 cm^{-1}. The tilt angle of the molecular chain with respect to the surface normal in a spontaneously formed monolayer has been determined to be 8.2° ± 1.8°.

Several studies have appeared that have explored both the tail and headgroup regions of the surfactant. Using the insoluble surfactant $CD_3(CH_2)_{19}CN$, Eisenthal and co-workers explored the orientation of the terminal deuterated methyl group and the polar nitrile group as a function of interfacial concentration.[137] For this Langmuir monolayer, the results indicate that the orientation of these two entities vary with surface concentration but in very different ways. It has been found that in the phase transition from the gas/liquid coexistence region to the liquid region, the spectral changes in the CN region are attributed to the breaking of hydrogen bonds with the CN group with the water squeezed out of the monolayer and subsequent reorientation of the headgroup. The orientation of the tail is found to be sensitive to the monolayer density even in the gas−liquid coexistence region with the tail becoming continuously upright upon compression. In another study of the tail and headgroup of surfactants, Watry and Richmond[138] examined the behavior of alkylbenzenesulfonate, a soluble surfactant, at both the vapor/water and CCl_4/water interfaces. The results are compared with related alkylsulfonates to learn how the presence of the benzene ring next to the sulfonate headgroup affects the behavior of the surfactant. The benzenesulfonate molecule studied, dodecylbenzenesulfonate (DBS), is a commonly used commercial surfactant and has been known to be several orders of magnitude more effective in reducing the surface tension of water relative to alkysulfonate surfactants. Figure 20 displays the spectrum of DBS at the vapor/water

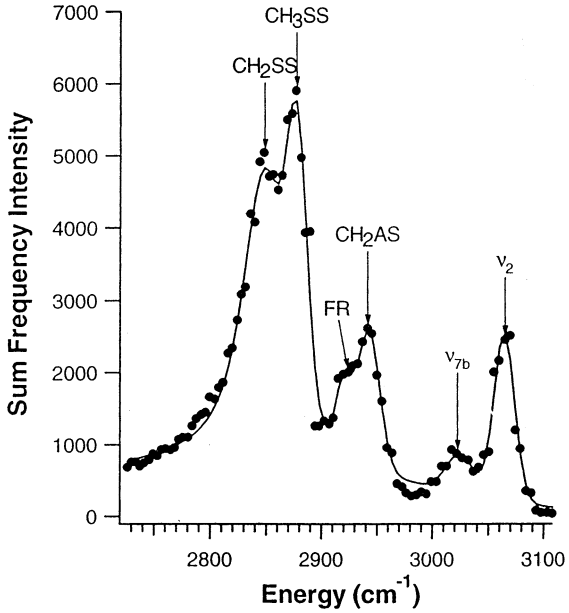

Figure 20. VSF spectrum of DBS at the air/D_2O interface. *SSP* polarization. The solid line is a fit to the data assuming a Voigt functional form for the peaks. (Reprinted with permission from ref 138. Copyright 2000 American Chemical Society.)

interface. The spectral peaks between 2800 and 2950 cm^{-1} correspond to the alkyl chain of DBS, whereas the modes above 3000 cm^{-1} correspond to the CH vibrational modes of the benzene ring. By monitoring the ratio of the intensity of the methylene and methyl CH stretch symmetric modes, they conclude that the alkyl chains of the DDS are highly disordered at the vapor/water interface as a function of concentration. Increased surface concentration from fractions of a monolayer to a full monolayer does not result in any increased ordering. In contrast, as the interfacial concentration of linear dodecylsulfonate increases at the vapor/water interface, the chain ordering increases indicative of increased chain−chain interactions. The authors attribute this difference in ordering to the presence of the benzene ring in DBS. The limiting surface area measurements and the orientation of the benzene ring, measured by monitoring the phenyl C−H modes as a function of concentration, support a picture that DBS exists at the interface in a staggered headgroup geometry. This picture is consistent with the benzene rings disrupting chain−

chain interactions for the first few methylene groups adjacent to the benzene ring in DBS. This staggered arrangement appears to significantly disorder the alkyl chains for DBS.

A study that combined second harmonic generation and VSF has demonstrated how molecular orientation and conformation of a surfactant chromophore can be measured at the vapor/water interface.[139] These studies have involved pentyl−cyanoterphenyl molecules for which three parts of the molecule have been examined upon adsorption. The cyano headgroup and pentyl chain has been examined by VSF, and the terphenyl ring has been examined by SHG. These molecules form a Langmuir monolayer on the water surface. The results give a quantitatively consistent picture of the molecular configuration if the appropriate refractive indices for the monolayer are used. They find that in order for their results to be physically reasonable and the deduced molecular conformation to be consistent with the commonly accepted one, a value of the index of refraction used must be different than that of a bulk phase value for the molecule and intermediate between the index of refraction of air and water. Using a value of $n' = 1.18 \pm 0.04$, they find that the molecules adsorb at the interface with a tilt angle of 51.5° ± 1.5° from the surface normal. Simple model calculations are used to justify the experimentally determined value of n'.

Bain and co-workers conducted the most extensive studies of a range of surfactants adsorbed at the vapor/water interface. One of their first studies involved measuring the vibrational spectrum of seven soluble surfactants adsorbed at this interface.[23] These included three nonionic surfactants (dodecanol, C_{12}-maltoside and $CH_3(CH_2)_{n-1}(OCH_2CH_2)_mOH$, or C_nE_m), the anionic surfactant sodium dodecyl sulfate, one zwitterionic surfactant (C_{12}-betaine), and two cationic surfactants, (C_{14} trimethylammonium bromide and didodecylammonium bromide). From the VSF spectra of the C−H stretch modes of the alkyl chains, the degree of conformational disorder and the angle of the terminal methyl group are inferred. They find that, in general, the number of gauche conformations increases as the area per chain increases. They also find that the angle of the methyl group, which is an indicator of the tilt of the hydrocarbon chains, is not simply related to the area per chain. A comparison of surfactants with the same chain length and area per molecule shows that the structure of the chain region of the monolayer is sensitive to the nature of the headgroup and not just to the packing density. A series of cationic surfactants has been the focus of another set of studies.[55,59,140−143] In a study that combines VSFS and neutron reflectivity, hexadecyltrimethylammonium *p*-tosylate has been examined. Single-chain cationic surfactants such as this form small spherical micelles in dilute solutions, but in the presence of aromatic counterions, they can transform into long, threadlike aggregates with dramatic effects on the optical properties and rheology of the solution.[144] In these vapor/water studies, they show that the aromatic anions cause major and unexpected changes to the structure of the monolayers.[141] They find that in order for the monolayer to generate space for the bulky tosylate ions, the area per surfactant molecule increases by about 25%. In a related study, the behavior of this cationic surfactant in the presence of a series of halide counterions has been examined by a combination of surface tension, ellipsometry, and VSFS. Neither the VSFS nor ellipsometry data provided any firm evidence for specific effects of the halide ions on the structure. The principal effect of the counterion is to change the efficiency and effectiveness of the surfactant (both decreasing in the order of $Br^- > Cl^- > F^-$). In another study, a series of alkyltrimethylammonium bromides ($CH_3(CH_2)_{n-1}N^+(CH_3)_3Br^-$), C_nTAB (n = 12, 14, 16, 18), has been examined at a constant area per molecule of 44 Å^2 to understand the effect of chain length on the molecular orientation. The data suggests that all four surfactants behave very similarly with a chain tilt of 58° near the methyl terminus. Complimentary ellipsometric data suggests that the density of the chain region in the monolayers is close to a liquid hydrocarbon. This and related neutron reflection data are consistent with the VSFS data.[143]

A study by Goates et al.[44] examined the conformational ordering of nonionic surfactants at the vapor/water interface. These nonionic surfactants that are in the category of alkyl poly(ethylene glycol) ethers, C_nE_m, are widely used as detergents, emulsifiers, and dispersants.[145] In these studies, the goal is to determine how the length of the poly(ethylene glycol) chain (EO) affects the structure of the monolayers when the length of the hydrocarbon chain is held constant. They find that for a constant headgroup area of 62 Å^2, the hydrophobic region of the monolayer has a density close to that of a liquid hydrocarbon and a structure that varies little with the length of the EO chain.

Mixed monolayers of surfactants and hydrocarbons have been the focus of several studies. A study of *n*-eicosane and a monolayer film of dodecanol at the vapor/water interface has been examined in the C−H stretch region by Sefler et al.[146] McKenna et al.[59] find that mixed monolayers of hexadecyltrimethylammonium bromide and tetradecane formed at the air−water interface exhibit a first-order phase transition from a conformationally disordered to a conformationally ordered state as the temperature is lowered. The phase transition occurs at approximately 11 °C above the melting point of tetradecane. A two-dimensional phase transition has been studied in a mixed monolayer of sodium dodecyl sulfate and dodecanol at the vapor/water interface.[147] They find with VSF and ellipsometry that at low temperatures, a monolayer at the surface of a solution containing 99.9% SDS and 0.1% dodecanol is conformationally ordered and has a surface coverage comparable to that of a monolayer of pure dodecanol at the same temperature. At 16 °C, a first-order phase transition to a phase that is less dense and more conformationally disordered is found. The high-temperature monolayer phase is more disordered than the corresponding liquid phase in pure dodecanol. The solid phase is found to contain equimolar amounts of SDS and dodecanol, whereas the liquid phase contains SDS and dodecanol in a ratio of 3:2. They attribute the

change in composition of the mixed monolayer to a reduction in the interaction parameter of the monolayer in the phase transition.

B. Water-Soluble Solutes Adsorbed at the Vapor/Water Interface

In recent years, a number of studies have appeared that examine the molecular structure of small water-soluble molecules at the vapor/water interface. The impetus behind most of these studies is to understand how atmospherically important molecules adsorb at this interface. Whereas atmospheric molecules have been studied extensively in the gas phase, very few spectroscopic studies have investigated these molecules on liquid surfaces. These studies provide new challenges for the VSF field due to the relatively low signal levels of these small molecules, the complexity in spectral interpretation due to interferences that can occur between various vibrational modes of the solute molecules and the water background, and the assignment of vibrational modes. Nevertheless, the surface sensitivity of the method and the applicability to the study of important heterogeneous reactions at a liquid surface makes the future bright for this area of research.

Air/acetonitrile−water interfaces have been the focus of two sets of studies. In the first set by Eisenthal and co-workers,[148,149] the VSFS measurements of this interface suggest a phase transition as the solution composition is varied. This is manifested in abrupt shifts in the CN vibrational frequency and orientation of acetonitrile molecules at the interface when the bulk acetonitrile (CH_3CN) concentration reaches 0.07 mole fraction. At lower concentrations it is found that the CN stretching vibrational frequency of acetonitrile at the interface is at a higher frequency than that of neat bulk acetonitrile (Figure 21a). At concentrations greater than 0.07 mole fraction acetonitrile in water, the frequency for surface acetonitrile molecules red shifts to a value that is near that of neat bulk acetonitrile. The spectral changes in the CN region are attributed to the breaking of hydrogen bonds with the CN group as the water is squeezed out of the monolayer with subsequent reorientation of the headgroup. The methyl group (measured with CD_3CN) does not exhibit any frequency change as a function of acetonitrile concentration as shown in Figure 21b. To develop a broader picture of this behavior the studies were followed by examination of air/proprionitrile−water and air/butyronitrile−water interfaces.[150] These molecules allow the study of the effect of the alkyl chain on the surface interactions which, for the acetonitrile case, are dominated by the hydrogen bonding of the CN with water and by the dipole−dipole interactions among CN units. For the butyronitrile system, no phase transition is observed with interfacial concentration. However, for proprionitrile, a phase transition as manifested by changes in CN frequency and CN molecular orientation is observed. The chain length dependence of the behavior is attributed to a lower interfacial packing density for molecules as the chain length increases. Huang and Wu examined the air/acetonitrile−water interface

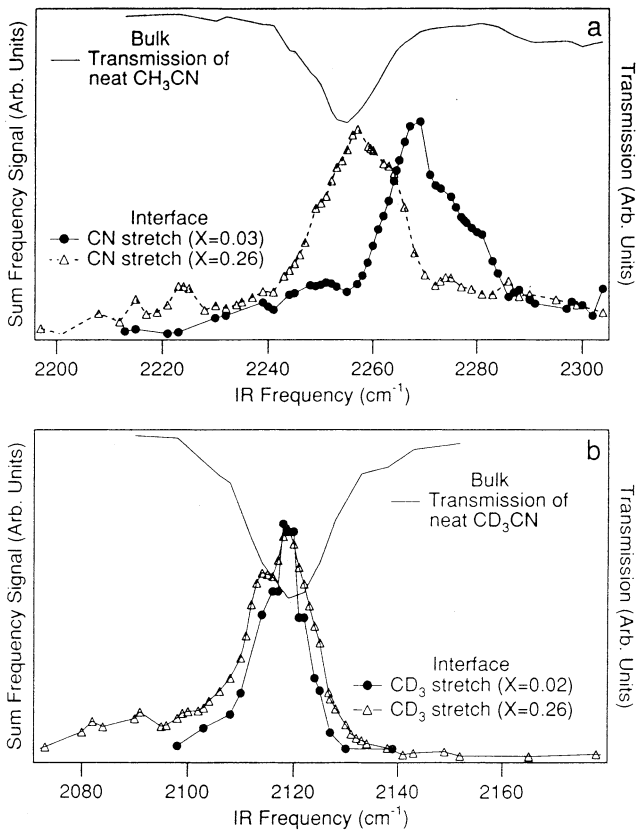

Figure 21. (a) Upper trace is a transmission spectrum of a neat bulk CH_3CN sample. The two bottom traces are sum frequency spectra of CN vibration in the air/solution interface at bulk mole fractions of $X = 0.03$ and 0.26. (b) The upper trace is a transmission spectrum of a neat CD_3CN sample. The two bottom traces are sum frequency spectra of the CD_3 symmetric stretch in the air/solution interface at bulk mole fractions of $X = 0.02$ and 0.26. (Reprinted with permission from ref 137. Copyright 1993 American Institute of Physics.)

and compared the behavior with the air/methanol−water interface.[151] These studies involved a combination of VSFS and third harmonic generation (THG). THG was used to obtain information about the microscopic structure of these liquids in the bulk medium. They found very different results for these two systems. For acetonitrile, the studies suggest the existence of microheterogeneity in the liquid mixtures with acetonitrile mole fractions higher than 0.3. This critical concentration for the bulk phase separation is larger than that appearing at the surface. For methanol, the polar distribution of the methanol molecules at the surface has been found to be enhanced by the interfacial water molecules.

Studies have been conducted on several sulfur-containing molecules examined at the vapor/water interface, specifically dimethyl sulfoxide (DMSO)[152,153] and methane sulfonic acid (MSA).[67] These molecules are present as trace constituents in the atmosphere. Recently, DMSO has been proposed as the heterogeneous precursor to atmospheric condensed phase MSA through an atmospheric cycle originating with dimethyl sulfide, a phytoplankton degradation product.[154−156] Aerosol particles containing MSA are thought to contribute to the class of aerosols which effectively scatter radiation out of the atmosphere. In the DMSO studies, the combination of surface

tension and VSF measurements show that for aqueous mixtures of DMSO and water, the DMSO molecules partition to the interface with a higher concentration at the surface than in the bulk. Figure 22a

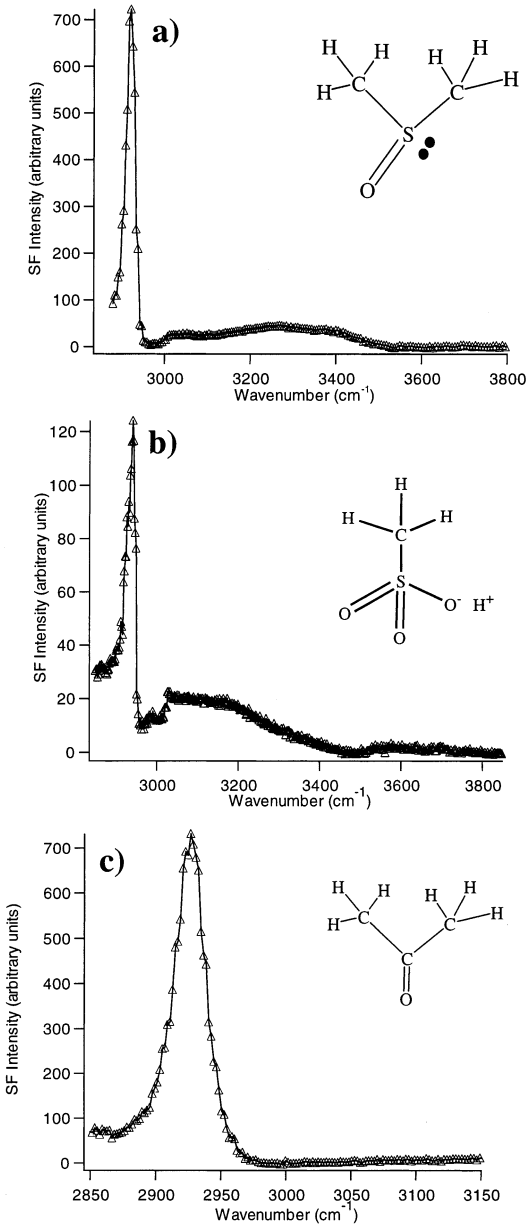

Figure 22. VSF spectra using *SSP* polarization of the surface of aqueous solutions containing (a) 0.1 mole fraction DMSO, (b) 0.1 mole fraction of MSA, and (c) 0.1 mole fraction of acetone. (Reprinted with permission from ref 152. Copyright 2000 Elsevier Science.)

shows a spectrum of an aqueous solution of DMSO at 0.1 mole fraction. The data were taken with *SSP* polarization. The sharp peak observed at 2920 cm^{-1} is assigned to the methyl symmetric stretch (SS) of DMSO. This peak is found to be shifted slightly to higher energy relative to the pure DMSO. The shift to higher energy has been attributed to a decreased interaction of the DMSO sulfur lone pair with the *trans*-CH of the methyl groups of DMSO. This decreased interaction is indicative of the changing orientation of DMSO with surface concentration as aggregation increases. This observation combined with changes in VSF intensity with DMSO surface concentration led to the conclusion that, as the surface concentration of DMSO increases, the DMSO molecules are aggregating and reorienting such that the two methyl groups are becoming more perpendicular to the solution surface. The methyl asymmetric stretch of DMSO appears as a small peak at 2990 cm^{-1}. This mode destructively interferes with the CH_3-SS[48,49] as determined when appropriate fitting procedures that take into account the phase relationship between these two modes are applied. This is visually manifested in spectrum Figure 22a as an asymmetry in the CH_3-SS mode and the dip in the spectrum near 2975 cm^{-1}. The large intensity of the SS mode relative to the AS mode indicates that the methyl groups are oriented predominately out of the interface.

Similar studies have been conducted with methane sulfonic acid.[67] The VSF spectrum of this molecule at the vapor/water interface is shown in Figure 22b. The CH_3-SS appears at 2940 cm^{-1} and the CH_3-AS appears near 3030 cm^{-1}. Once again, the strong asymmetry in the CH_3-SS peak is due to the destructive interference between the two methyl stretching modes. The VSF intensity centered around 3100 cm^{-1} is attributed to the cooperative intermolecular hydrogen-bonding modes of surface water (see earlier discussion). Unlike DMSO, as the MSA surface concentration is increased from low bulk concentrations to pure MSA, the frequencies of both CH_3 modes do not shift. Additionally, the SF intensity tracks with the surface number density obtained from surface tension measurements, leading to the conclusion that unlike DMSO, the methyl group of surface MSA does not reorient as a function of surface concentration. It is interesting to compare the VSF spectrum of these molecules with water/acetone studies.[152] Acetone, ubiquitous in many regions of the atmosphere, has recently been shown to be the second highest concentration organic trace-gas constituent next to methane in regions of the Northern Hemisphere. It is believed that it may play a role in the growth and surface chemistry of atmospheric aerosols.[156] Figure 22c shows the spectrum of acetone at an aqueous 0.1 mole fraction solution and a temperature of 15 °C.[152] The CH_3-SS mode appears for acetone at 2926 cm^{-1}, which is slightly shifted from the bulk Raman and IR studies which place it at 2922 and 2924 cm^{-1}, respectively.[157] The CH_3-AS is less distinct, primarily due to the narrow separation between these two peaks for acetone (~43 cm^{-1}) relative to DMSO (~84 cm^{-1}) and MSA (89 cm^{-1}). The surface methyl groups of acetone preferentially orient away from the bulk liquid. VSF studies of pure acetone surfaces have been reported[157] with results similar to the aqueous acetone studies of Allen et al.[152] These studies were conducted at three polarizations, *SSP*, *PPP*, and *SPS*. These studies, which combine VSF measurements and molecular dynamics simulations, suggest that one of the methyl groups points away from the liquid surface and the other is embedded in the liquid. The assignment of the CH_3-SS mode and its energy agrees well with the earlier work of Allen et al.,[152] although the destructive

interference and assignment of the CH_3−AS is not specifically addressed. The acetone surface is concluded to be more ordered than that of the bulk.

Ammonia−water complexes have been the focus of work by Shultz and co-workers.[81,158] Understanding the interaction of ammonia with different surfaces arises from its importance in heterogeneous catalysis and its relevance to various industrial processes. With ammonia as the most abundant alkaline compound in the atmosphere, it is the principal species that neutralizes strong inorganic acids and hence is important in atmospheric chemistry.[159] Figure 23

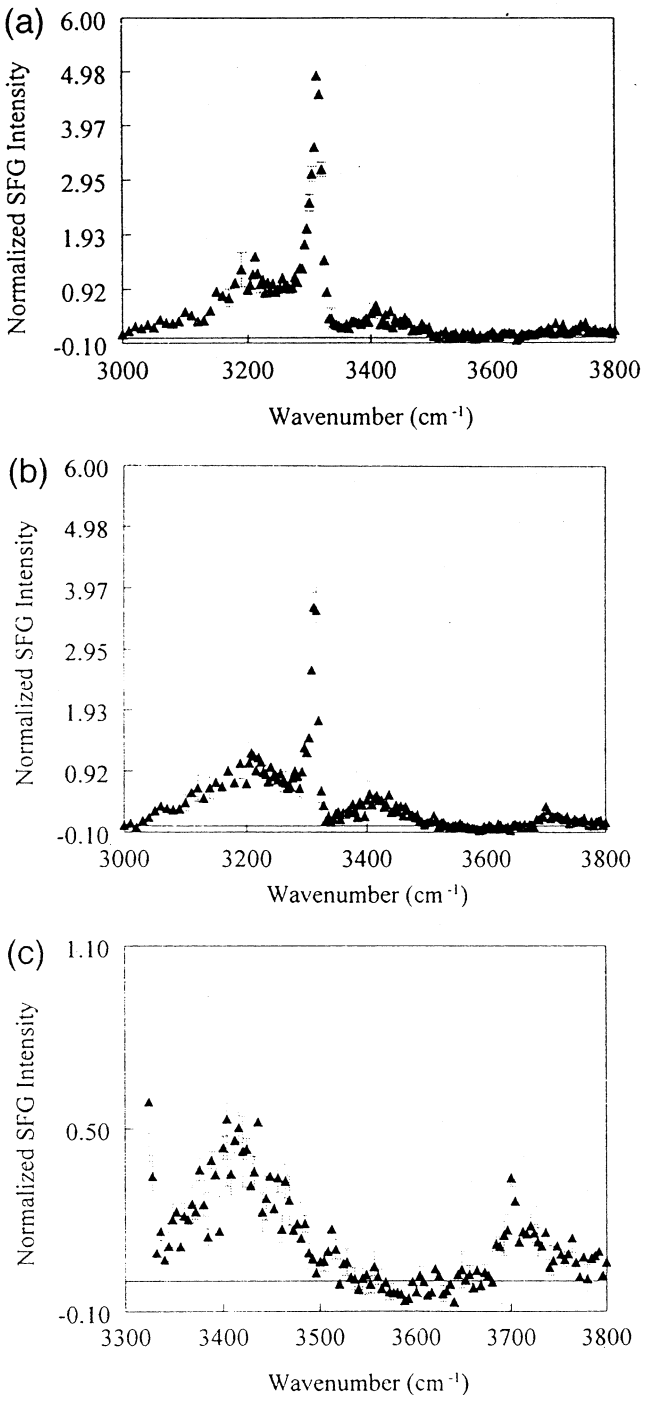

Figure 23. (a) VSF spectrum of concentrated ammonia using *SSP* polarization and solutions of decreasing ammonia concentration (b and c). (Reprinted with permission from ref 81. Copyright 1998 Elsevier Science.)

shows a VSF spectrum of concentrated ammonia. The major feature in the spectrum at 3312 cm^{-1} is an intense peak assigned to the symmetric N−H stretch, confirming the presence of NH_3 at the interface. This peak is red shifted by ~20 cm^{-1} from the fundamental NH_3 infrared gas-phase absorption. A weaker deformation mode is observed at 3200 cm^{-1}. The dangling (free) OH peak is suppressed due to water molecules complexing with ammonia at the interface. In increasingly dilute ammonia solutions, the N−H SS mode is less intense and the free OH peak of water appears. Comparison of the calculated and observed VSF intensities for different polarization combinations has been used to determine the tilt angles for surface ammonia molecules, further characterizing the structure of the ammonia complex. Figure 24 is a schematic of the NH_3−H_2O complex

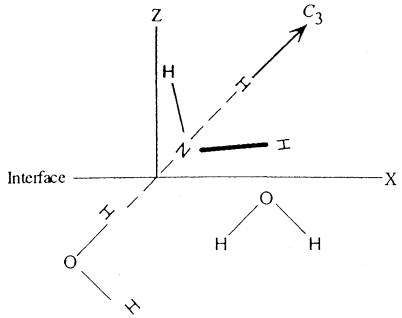

Figure 24. Schematic of the NH_3−H_2O complex orientation with respect to the surface *XYZ* axis. The C_3 molecular axis is approximately 38° from the surface normal *Z*. (Reprinted with permission from ref 158. Copyright 2000 American Institute of Physics.)

orientation derived from these studies. The C_3 axis is concluded to be tilted between 25° and 38° relative to the surface normal and a twist angle of ≥10°. The orientation analysis yields an average configuration. The authors examine the influence of the local dielectric constant and the contributions of the Raman transition polarizability tensors on the orientation analysis but find that these do not affect the conclusions about orientation.

C. Surfactants Adsorbed at Organic/Water Interfaces

1. Charged Alkyl Surfactants

Understanding the molecular structure of adsorbates at the interface between two immiscible liquids provides new challenges for both experimentalists and theorists. Few molecular studies to date have been conducted at the interface between an aqueous phase and an organic or hydrophobic liquid phase that provide information about how surfactants or adsorbates orient and structure as they adsorb. The first and the majority of these studies to date have been conducted using VSFS.[160,161] Whereas the studies of liquid/liquid interfaces described above focus on water structure and how it is affected by the adsorbates, in this section, the focus is on the adsorbate structure and in some cases how this molecular structuring compares with similar adsorption at a vapor/water interface.

The first successful measurements of the vibrational spectroscopy of alkyl charged surfactants adsorbed at a liquid/liquid interface have been reported by Messmer et al.[57] The goal of these VSFS studies has been to measure the vibrational spectrum of a simple surfactant, SDS, at this interface to understand how such surfactants orient and assemble, similar to the above-described vapor/water studies. As mentioned earlier, the success of these otherwise low signal experiments has come from the design of appropriate cells to allow the experiments to be conduced by TIR. Carbon tetrachloride and D_2O have been used in these experiments as well as later ones because of their transparency to the infrared light around 3 μm where the CH stretch modes of the surfactants appear. These studies demonstrated that spectra of SDS could be readily obtained at this interface. Analysis of the acquired spectra show that for a monolayer of SDS there is considerable disorder in the alkyl chains at all interfacial concentrations. Later more detailed studies examined both hydrogenated and deuterated SDS to allow more accurate spectral assignments of CH stretch modes in these and previous vapor/water studies.[54] This study also examined the chain ordering and the terminal methyl group orientation of SDS as a function of interfacial concentration. As in previous studies, the ratio of the methyl/methylene intensity has been used to determine molecular conformation. The studies were accompanied by surface tension measurements to allow correlation of the VSF signal and interfacial concentration. The studies show that at all interfacial concentrations the surfactants display considerable conformational disordering. On average, the chains are oriented normal to the interface. As the concentration increases, the chains show increased ordering. However, the persistence of the methylene signal indicates that the chains never reach the all-trans configuration that is seen for monolayers at vapor/water or air/solid interfaces. This disorder has been attributed to the presence of the CCl_4 penetrating into the chains and disrupting the van der Waals interactions between the chains.

In a related series of studies surfactants of differing charged headgroups[54,162] and chain lengths have been examined at the CCl_4/D_2O interface. In the former, SDS, sodium dodecylsulfonate (DDS), dodecylammonium chloride (DAC), and dodecyltrimethylammonium chloride (DTAC) have been studied as a function of interfacial concentration and optical polarization. As with the previous SDS study,[57] all indicate the presence of gauche defects in the hydrocarbon chain as determined from the intensity ratio of the methyl to methylene symmetric stretch vibrational modes. An increase in the surface concentration results in a reduction of gauche defects in the hydrocarbon chain. The spectra suggest that the conformational ordering is different for the cationic versus anionic surfactants. The alkyl chains of the cationic surfactants possess the fewest gauche defects, whereas the anionic surfactants display more disorder in the hydrocarbon chains at similar surface concentrations. In studies of chain length, the conformational ordering of three alkanesulfonates have been examined, sodium hexanesulfonate (HS), sodium undecanesulfonate (UDS), and sodiumdodecanesulfonate (DDS) adsorbed at the D_2O/CCl_4 interface.[162] For all, an increase in interfacial concentration leads to a reduction of gauche defects in the hydrocarbon chains. The alkyl chain of HS displays the fewest gauche defects, while DDS and UDS display more disorder in their hydrocarbon chains at similar surface concentrations. This is interpreted as a reduction in the possible number of gauche conformations in the shorter alkyl chains.

Both the headgroup and the chains of a charged surfactant at the CCl_4/H_2O interface have been examined in a study of sodium dodecylbenzene sulfonate (DBS) where the orientation of the headgroup has been examined by monitoring changes in phenyl CH mode intensities.[138] DBS is an important industrial and commercial surfactant used in cleansers and detergents. VSFS studies have been conducted at both the vapor/water and CCl_4/D_2O interfaces with the former studies described in section IV.A. The results have been compared with sodium dodecylsulfonate (DDS), which has the same alkyl chain length. DDS exhibits typical simple surfactant behavior found in the previous VSF studies.[163] Figure 25 shows a plot of the ratio of methyl/methylene SS for the these systems. For the DDS (Figure 25a), there is a rise in the ratio with surface concentration indicative of increased order with concentration until monolayer coverage results in a more constant value. In contrast, at the vapor/water and CCl_4/water interface (Figure 25b and c, respectively), DBS does not undergo any ordering of the chains as monolayer coverage is approached. The chains are highly disordered at all surface concentrations at both interfaces. Even in the presence of excess salt, which screens the charged headgroups and allows the DBS molecules to pack more tightly, there is no significant change in the order of the alkyl chains (Figure 25d). The authors attribute this to the disruptive nature of the bulky phenyl group in DBS that does not allow the alkyl chains to order as well as DDS. Phenyl group orientation for DBS has been examined by following the strongest phenyl mode (analogous to ν_2 in benzene) which has its IR transition moment pointing from the alkyl chain to the sulfonate. Figure 26 shows the SF intensity dependence on surface concentration for the phenyl CH modes at the two interfaces. For the vapor/water interface, the minimal change in intensity at low concentrations followed by a sharp rise as a monolayer is achieved suggests that there is an abrupt change in orientation of the phenyl group as the interface reaches a high level of packing. For the liquid/liquid interface the linear relationship between the square root of the intensity and the surface concentration indicates minimal reorientation with concentration. Polarization studies indicate that the phenyl groups are oriented perpendicular to the interface throughout this concentration range. The combined observations described and the results from surface tension measurements showing that the headgroup areas at monolayer coverage for DDS and DBS are nearly the same, suggest that the phenyl rings are in a staggered arrangement at the liquid/

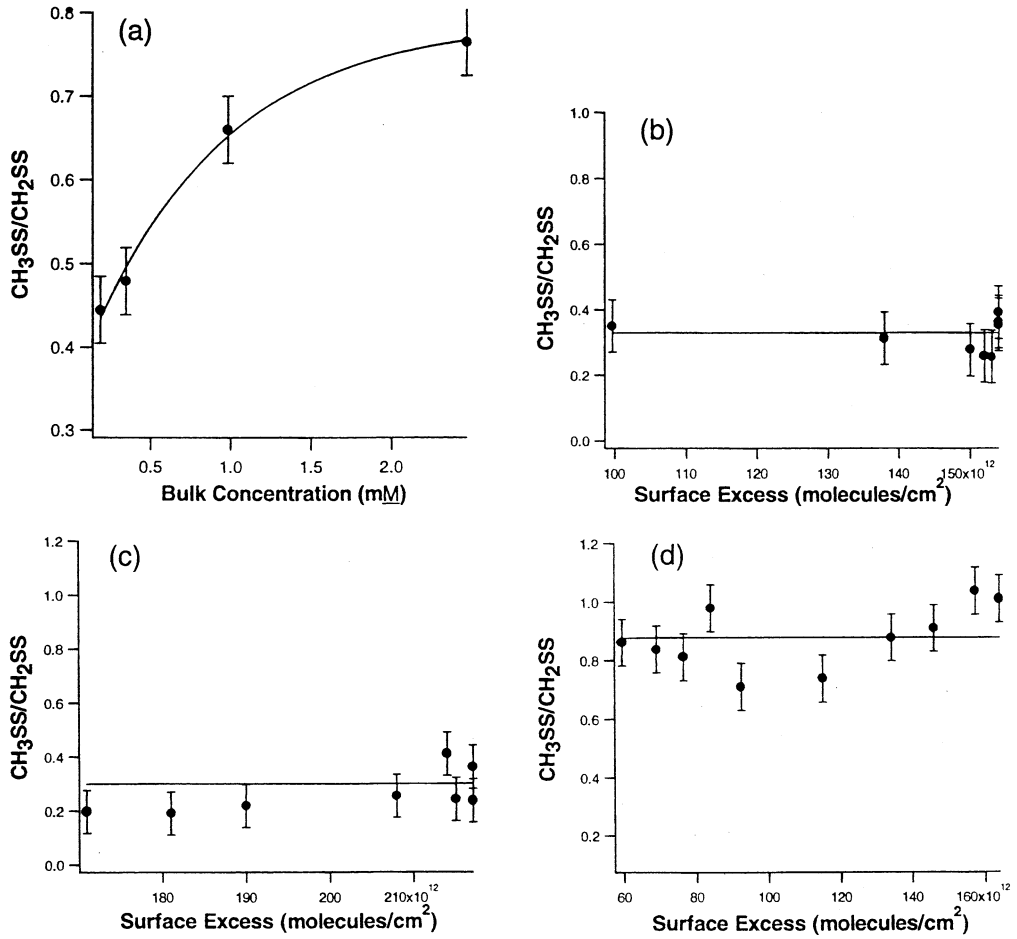

Figure 25. Ratio of the methyl to methylene symmetric stretch intensities as a function of surface concentration for (a) DDS at the air/water interface, (b) DBS at the air/water interface, (c) DBS at the air/water interface with 0.1 M NaCl, and (d) DBS at the CCl_4/water interface with 0.1 M NaCl. (Reprinted with permission from ref 138. Copyright 2000 American Chemical Society.)

liquid interface and that this staggering of the headgroups disrupts the ability of the chains to order while allowing the phenyl rings to maintain their perpendicular orientation.

2. Biomolecules

Many important biomolecules in biological organisms and in the environment are classified as surfactants because of their tendency to adsorb at hydrophobic/hydrophilic interfaces. Phospholipids are one example of such biological surfactants. These biomolecules constitute the major component of most cell membranes and consist of a charged headgroup connected to a pair of long acyl chains by means of a three-carbon glycerol backbone. At interfaces, these amphiphilic molecules form Langmuir films which exhibit a host of different phases and morphologies.[164,165] The interest in studying their behavior at liquid surfaces arises from the ability to use any insight gained from these studies to understand the nature of more complex phase behavior which takes place in bilayer systems. Most previous studies of phospholipid assembly using other methods have been conducted at vapor/water interfaces.[165,166]

The molecular structure of phospholipids assembled at the vapor/water and organic/water interfaces has been studied in a number of VSFS studies. The first VSF studies of phospholipids at an organic/water interface were reported by Walker et al.[167] In these experiments, spectra of the CH stretching region of several different phosphocholines adsorbed to the D_2O/CCl_4 interface were measured. As with other surfactants, the relative intensity of the CH−SS modes have been used as a means of determining chain conformation. The phospholipids used belong to a class of saturated, symmetric, dialkylphosphocholines (PCs) having alkyl chain lengths of 12 carbon atoms (dilauroyl-PC or DLPC), 14 carbon atoms (dimyristoyl-PC or DMPC), 16 carbon atoms (dipalmitoyl-PC or DPPC), and 18 carbon atoms (distearoyl-PC or DSPC) (Figure 27). These monolayers formed from the breakup at the interface of aqueous phase phosphocholine vesicles with their adsorption measured by VSFS in conjunction with interfacial tension measurements. The experiments were conducted at a series of concentrations above and below the bilayer gel to liquid crystalline phase transition temperature. It has been found that chain order is dependent on both alkyl chain length and interfacial phospholipid concentration. The interfacial pressure studies show that the forces within the bilayers of the aqueous vesicles control the interfacial concentration at the liquid/liquid interface and hence of the subsequent conformation of the adsorbed PCs.

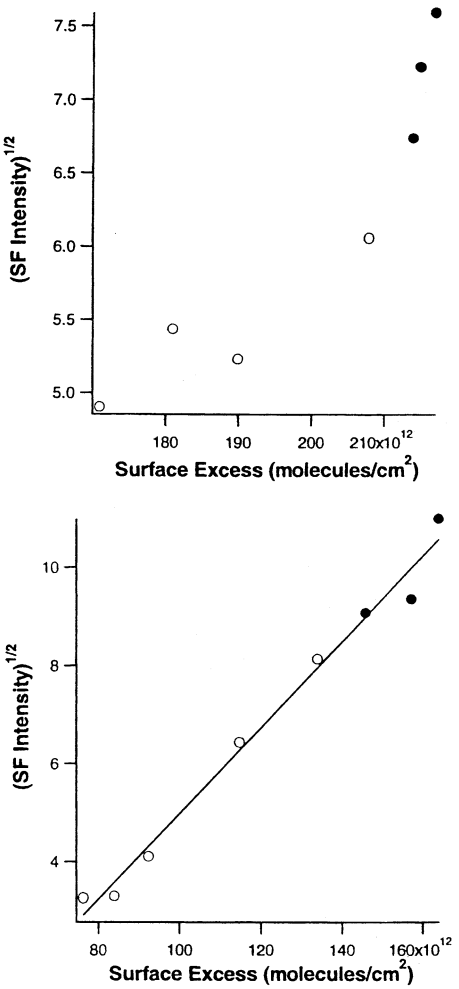

Figure 26. Square root of the VSF intensity of the ν_2 mode as a function of concentration for (a) DBS at the air/water interface with 0.1 M NaCl and (b) DBS at the CCl_4/water interface with 0.1 M NaCl. The solid data points correspond to concentrations where surface pressure measurements indicate maximum surface coverage. (Reprinted with permission from ref 138. Copyright 2000 American Chemical Society.)

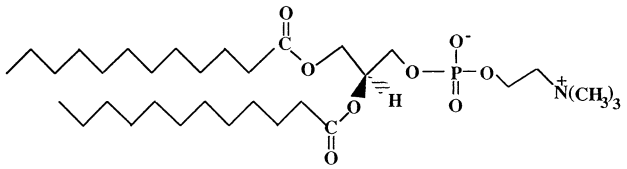

1,2-Dilauroyl-sn-Glycero-3-Phosphocholine (DLPC, C_{12})

Figure 27. Phospholipids used belong to a class of saturated, symmetric, dialkylphosphocholines (PCs) having alkyl chain lengths of 12 carbon atoms (dilauroyl-PC or DLPC), 14 carbon atoms (dimyristoyl-PC or DMPC), 16 carbon atoms (dipalmitoyl-PC or DPPC), and 18 carbon atoms (distearoyl-PC or DSPC). (Reprinted with permission from ref 118. Copyright 1999 Elsevier Science.)

For PCs originating from the liquid crystalline state of vesicle bilayers, the reduced barrier to vesicle breakup at the interfaces results in a higher degree of order among the alkyl chains. In contrast, stronger cohesional forces in the vesicles in the gel state inhibit PC deposition at the interface and the alkyl chains of these expanded monolayers show greater disorder. At equivalent interfacial concentration, the alkyl chain structure of the PCs show a dependence on chain length. At the vapor/water interface, monolayers composed of longer chain phospholipids show greater alkyl chain ordering than the shorter chain PCs. For the same PCs studied at the water−CCl_4 interface, there is much less of a difference in ordering with chain length and, in fact, there is a slight trend toward decreased chain ordering with chain length. The authors interpret this difference as evidence that under ambient conditions the CCl_4 solvates the alkyl chains of monolayers adsorbed at the water−CCl_4 interface. Monolayers consisting of longer chain species (i.e., DPPC and DSPS) are more readily solvated than the shorter chains, and the reduction in interchain attractive forces leads to greater propensity for torsional distortion and gauche defects. Similar chain length studies have been conducted for comparison at the vapor/water interface.[168,169] For the vapor/water interface, the longer chains are more conformationally ordered as they experience stronger interchain van der Waals forces and form monolayers corresponding to more ordered monolayers than those of their shorter chain counterparts. A later study in this laboratory extended these studies of symmetric PCs to those with longer alkyl chains up to C_{22}.[170] Different methods of monolayer preparation have been necessary in these studies due to the insolubility of the larger PCs in the aqueous phase. Samples were prepared by dissolving the PC in chloroform and spreading it at the interface by gently expelling small drops of the chloroform solution from a syringe tip placed underneath the vapor/water interface above the liquid/liquid interface and allowing them to fall by gravity to the liquid/liquid interface. Several sample spreadings were necessary in some cases to produce the desired close-packed interfacial monolayer at the liquid/liquid interface. With this means of preparation it has been found that the C_{18} and longer chain PCs form extremely well-ordered interfacial layers with chains in a predominately all-trans conformation while C_{16} and C_{15} PCs formed layers with disordered chains. The C_{17} PCs produced layers with intermediate degree of order.

In another set of VSF studies of PCs, Smiley and Richmond examined the molecular level organization of saturated symmetric and asymmetric chain PCs.[171] The importance of this study is that a large majority of biological phospholipids contain two dissimilar hydrocarbon chains per molecule. Little is known about asymmetric chain phospholipids in bilayers, and even less is known about their monolayer properties. In these studies the PC monolayers have been formed at the CCl_4/H_2O interface by injection of PCs into the bulk aqueous phase. The PCs had varied chain combinations of C_nC_m where n = 18, 16, 14, and 12 and m = 18, 16, 14, 12, and 10. It has been found that three of the PCs studied, specifically C_{18}/C_{16}, C_{18}/C_{18}, and C_{16}/C_{18}, formed extremely well-ordered layers with primarily all-trans chain conformations. Highly asymmetric PCs showed relatively disordered chains as might be expected from the reduced chain−chain interactions among the mismatched portions of the longer chains. The shorter

chain PCs of <16 carbons/chain are also relatively disordered. The authors attribute the greater disorder seen in the shorter chain PCs, irrespective of chain mismatch, as a consequence of reduced chain−chain interactions relative to the longer chain PCs. Interestingly, the main differences measured in these films could not be predicted based on the respective gel-to-liquid crystalline phase transition temperatures. Disordered chains were found for PCs both above and below their respective transition temperature for these room-temperature studies. The authors speculate that this may result from interfacial layer subtransitions.

A series of studies of biological systems has been conducted by Cremer and colleagues that examined biomolecules, including proteins, as they adsorb at quartz surfaces. These recent studies shed light on how water structures near these biological macromolecules under various pH conditions.[172−175]

D. Surfactants and Adsorbates at Solid/Aqueous Interfaces

Studies of molecular structure of solid/liquid interfaces provide further application for VSFS.[52] Several studies have appeared that explore the structure of monolayers and surfactants at a solid/water interface. Bain and co-workers examined the coadsorption of SDS and dodecanol a model hydrophobic surface that was prepared by self-assembly of octadecanethiol (ODT) on gold.[176,177] In the first study,[176] they show that VSFS could discriminate between the coadsorbed SDS and dodecanol and demonstrate the sensitivity of VSFS to the packing density and conformational order in the adsorbed monolayer. Selective deuteration has been employed to distinguish between the two adsorbed surfactants. In the second study,[177] with quantitative measurements of mixed monolayers, it has been found that dodecanol partitioned to the interface at a higher level than present in the bulk liquid. For example, a mixture of 6 mM SDS + 10 μM dodcanol showed a monolayer comprised of 63% dodecanol and 37% SDS. It had a packing density comparable to that of a pure monolayer of dodecanol. The composition of the monolayer has also been found to be isotope dependent. It is suggested that the dependence arises from a highly surface active impurity in the SDS or quantitatively by a lattice model of the monolayer within regular solution theory. Briggs et al.[178] measured the adsorption of a series of dichain sugar surfactants (di-(C_n-Glu)) from an aqueous solution onto a similar deuterated ODT surface chemisorbed on a gold-coated, chromium-primed silicon wafer. By monitoring the ratio of methyl and methylene SS modes they determined the relative conformational ordering in the di-(C_n) chains. The SF spectra show that for di-(C_6-Glu), the effectiveness and efficiency of adsorption is only marginally affected by temperature up to 95° C. Using partially deuterated d_{30}-di-(C_6-Glu) monolayers, they show that methylene resonances arise solely from the tail groups. The methylene mode amplitudes are found to generally increase with di-(C_n-Glu) tail length as a result of more gauche defects. The methyl mode amplitudes remain nearly constant. Conformational disorder in the tail group is found to increase with decreasing solution concentration and solution concentration below the critical micelle concentration. The monolayers show exceptional thermal stabilities on hydrophobic surfaces. This makes them attractive candidates for forming temperature-insensitive microemulsions with application in enhanced oil recovery. Zolk and co-workers[179] investigated the solvation of olio(ethylene glycol)-terminated self-assembled monolayers on gold in the C−H stretching region. Comparison of the monolayers in ambient atmosphere, in contact with water, and in contact with carbon tetrachloride show that the film structure is strongly disturbed by the interaction of the liquid with the monolayer. These results are consistent with the earlier conclusions of monolayers at the CCl_4/H_2O interface.[54,161,167,180] In related studies of dioctadecyl dimethylammonium chloride (DOAC) adsorbed at quartz/liquid interfaces, it has been found that the chains can assume many different conformations depending upon whether the solvent is CCl_4 or $CDCl_3$, short-chain alkanes, alcohol, or water.[180] Duffy and co-workers examined the adsorption of potassium oleate and sodium octanoate at the iron−water interface.[181] These studies are important because of the use of lubricating films to reduce friction at metal surfaces. The molecules studied are believed to act as boundary layer lubricants at iron surfaces in aqueous solution. The strength and phase of the resonances in the VSF spectrum of oleate indicate that a bilayer was adsorbed at the iron surface. In comparison, adsorbed sodium octanoate did not contain any resonances at any applied potential implying that the ordered films formed by oleate are more effective at lubricating than the disordered films.

E. Electrochemical Interfaces

VSF measurements metal/aqueous electrode surfaces have thus far been conducted on Au, Ag, and Pt electrode surfaces. The most extensive studies have been conducted with platinum single-crystalline and polycrystalline surfaces. Using a free electron laser, Guyot-Sionnest and Tadjeddine demonstrated the first use of VSFS to study ionic adsorption at an electrified metal/aqueous electrolyte interface.[182,183] These studies involved measurements of cyanide (CN^-), thiocyanate (SCN^-), and carbon monoxide (CO) adsorbed on polycrystalline platinum. The studies indicate that the CN^- and SCN^- adsorb at the surface but that the nitrogen atom can take two different orientations, either facing or pointing away from the surface. Daum and co-workers using a broadly tunable IR laser system conducted similar experiments on Pt(111) and found evidence for covalently bound CN^-.[184−186] The adsorption of CN^-, SCN^-, and related OCN^- ions has also been examined on Ag and Au electrodes where the adsorption is found to vary with potential in characteristic ways for each of the ions.[187−190] Hydrogen adsorption on polycrystalline and single-crystal Pt electrodes has been examined in several studies by Peremans and Tadjeddine.[187,191−194] In these studies a significant potential dependence in the VSF spectrum of the

Pt−H stretch is found. More than one peak for this mode appears, which the authors attribute to the bonding. The same investigators also examine the electrochemically induced decomposition of methanol on Pt electrodes using VSFS by monitoring the CO adsorption after decomposition.[187,195−197] The CO has been found to be present in both a single and multiple bonded state. The lifetime of a CO stretch vibration on a Pt surface has also been examined and found to be a few picoseconds.[198−200] This lifetime is found to be relatively independent of the solvent environment or the application of electrochemical potential. The orientation of acetonitrile at the Pt(111) electrode has been examined as a function of concentration and electrode potential.[201] Acetonitrile is found to orient with applied potential with the C−C bond perpendicular to the surface. Between 200 and 600 mV (vs the normal hydrogen electrode) its orientation is predominately with the methyl group directed toward the metal while the CN group is toward the metal above 800 mV. As water is added to the solution, the orientation is found to be disrupted.

F. Polymer Surfaces

Several studies have appeared that investigate the properties of water at polymer surfaces.[202−204] Kim and Shen[204] studied the treatment of polyimide surfaces treated with NaOH solution to improve the adhesion with metals. Both ultraviolet absorption and VSFS have been employed in the studies. They found that the conversion and subsequent etching of the polyimide film by the solution is more effective in the amorphous part of the film. Drying of the film converts the surface amides back to imides. In studies of the water/poly(ethylene glycol) interface, Dressen et al.[202] show that poly(ethylene glycol), whose molecular arrangement is originally relatively ordered, becomes disordered in the presence of water. Additionally, they find a new OH band that they identify to water molecules that are strongly interacting with the polymer. Three polymer blends immersed in water have been examined in studies by Gracias et al.[203] using both VSFS and scanning force microscopy. These studies involved polyethylene and polypropylenes of different molecular weights and structures. In aqueous solutions, polymer blends were found to segregate with the more hydrophilic polymer going to the surface. These studies have relevance to understanding the hydrated state of biopolymers that can be used as implants in the body.

V. Summary and Conclusions

There has long been a desire to understand the molecular structure and bonding that occurs at aqueous surfaces and interfaces. It is only recently that experimental techniques have become available to provide this type of information. Vibrational sum frequency spectroscopy is increasingly becoming a tool of choice for such studies because of its ability to measure the vibrational spectroscopy of molecules with inherent surface specificity, and the ability to make such measurements in a conventional laboratory setting. The future is particularly promising in this area as studies proceed to longer wavelengths where different adsorbate modes can be measured, and to shorter time scales where interfacial dynamics can be probed. This review has provided an overview of VSFS studies that have been conducted on aqueous surfaces and the contributions that the results have made to the field.

As this review describes, the molecular structure and bonding of water at a vapor/water interface has been the most extensively studied system since the first measurement was made by VSFS nearly a decade ago. Recent advances in laser technology and detection methods, inclusion of appropriate normalization procedures for power and anomalous dispersion, and improved sample preparation are resulting in a consensus from various laboratories as to the most accurate spectrum of OH stretching modes from the vapor/water interface. The current challenge is obtaining an interpretation of this spectrum that involves identification of different types of water bonding species at the interface. This requires attention to appropriate analysis procedures and spectral fitting routines that take into account the phase relationships between contributing vibrational modes and interferences between adjacent resonant modes and orientational effects. Important input in deconvolution of broad spectral features, such as polarization and isotopic dilution experiments, are providing valuable new information. Equally important are theoretical treatments of this and other aqueous interfaces that assist in interpretation of the data via the molecular simulations and simulation of VSF spectra. Studies of the adsorption of small solute molecules that have relevance to atmospheric process are also being studied at these surfaces, and important information about the partitioning and structuring at the vapor/water interface is emerging. There are a plethora of molecules and systems that will be valuable to study in this area in order to understand reactions and the molecular structure of the surfaces of aerosols and other aqueous surfaces. Beyond the room-temperature vapor/water interface, VSF offers exciting opportunities for understanding ice surfaces and ice/water interfaces as a function of temperature, different ice crystal faces, and thin films of ice grown on different solids. The VSF studies will provide important surface-specific input to add to information from a growing number of techniques that are providing insight about molecular structure and interactions at ice surfaces.

The structure and bonding of water in contact with a hydrophobic liquid is an area that has been largely dominated by theoretical efforts due to the paucity of experimental methods for probing this complex interface. This review demonstrates the type of information that can be gained from VSFS studies in this area. VSFS has recently provided the first detailed molecular insight into contributing water species at this type of interface, first at the CCl_4/H_2O interface and now with the extension to other hydrocarbon/water interfaces. The studies show weaker bonding interactions between interfacial water molecules than at the vapor/water interface and also show evidence for the importance of the interfacial

potential created by attractive interactions between water dipoles and the polarizable organic fluid. Isotopic dilution studies and analysis procedures that appropriately take into account the molecular orientation and the phase relationships between contributing OH modes and the weaker bonding nature of this interface have allowed spectral assignments and spectral fitting to be done at a level beyond what has been previously possible in VSF spectra of water. The CCl_4/H_2O studies provide the framework for future studies of organic/water interfaces that hold much promise in future years. These experimental efforts will benefit from theoretical efforts in this area that are just beginning to appear. As an extension of these neat liquid/liquid studies, related VSFS studies of these interfaces in the presence of trace charged species at the interface demonstrate the sensitivity of this technique to water molecules solvating charge at this interface. Future studies will be important in this area, particularly as it relates to an improved understanding of charged species at hydrophobic surfaces.

The review has also described the growing number of studies that have examined the adsorption of molecules and surfactants at aqueous interfaces including vapor/water, organic/water, and solid/water interfaces. These studies conducted largely at both vapor/water and liquid/liquid interfaces have largely focused on the conformation and ordering of alkyl groups on the adsorbates. As lasers with broader wavelength capabilities in the infrared become more prevalent and studies move beyond the C−H and N−H stretch modes of most current studies, valuable information will be gained about other parts of these molecules, particularly regions that reside at the aqueous surface. There are numerous biologically important interfacial processes involving surfactants and solutes that would benefit from VSF studies that have important relevance to respiration, anesthetics, ion transport, and macromolecular assembly. The same is true for the study of surfactants involved in remediation, oil extraction, lubrication, and commercially important products. At solid/liquid interfaces, including electrochemically relevant systems, there are many important issues to examine about the solvating layer at these solid surfaces and all types of adsorption including potential-induced adsorption.

VI. Acknowledgment

The author acknowledges the financial support for the range of studies from her laboratory described in this review. These agencies include the National Science Foundation (CHE-9725751) for the studies of water at various interfaces, Basic Energy Sciences of the Department of Energy for the atmospheric studies, the Office of Naval Research for the biomolecular studies, and the Petroleum Research Fund of the American Chemical Society for the surfactant studies.

References

(1) Stillinger, F. H.; Ben-Naim, A. *J. Chem. Phys.* **1967**, *47*, 4431.
(2) Stillinger, F. H. *Science* **1980**, *209*, 451.
(3) Hummer, G.; Garde, S.; García, A. E.; Paulaitis, M. E.; Pratt, L. R. *J. Phys. Chem. B* **1988**, *102*, 10469.
(4) Hummer, G.; Garde, S.; Garcia, A. E.; Pratt, L. R. *Chem. Phys.* **2000**, *258*, 349.
(5) Lum, K.; Chandler, D.; Weeks, J. D. *J. Phys. Chem. B* **1999**, *103*, 4570.
(6) Wilson, M. A.; Pohorille, A.; Pratt, L. R. *J. Phys. Chem.* **1987**, *91*, 4873.
(7) Sokhan, V. P.; Tildesley, D. J. *Mol. Phys.* **1997**, *92*, 625.
(8) Weeks, J. D. *J. Chem. Phys.* **1977**, *67*, 3106.
(9) Townsend, R. M.; Rice, S. A. *J. Chem. Phys.* **1991**, *94*, 2207.
(10) Croxton, C. A. *Fluid interfacial phenomena*; Wiley: New York, 1986.
(11) Benjamin, I. *J. Chem. Phys.* **1992**, *97*, 1432.
(12) Benjamin, I. *Science* **1993**, *261*, 1558.
(13) Lee, S. H.; Rossky, P. J. *J. Chem. Phys.* **1994**, *100*, 3334.
(14) Silverstein, K. A. T.; Haymet, A. D. J.; Dill, K. A. *J. Am. Chem. Soc.* **1998**, *120*, 3166.
(15) Schweighofer, K. J.; Benjamin, I. *Chem. Phys. Lett.* **1993**, *202*, 379.
(16) Shen, Y. R. *Solid State Commun.* **1998**, *108*, 399.
(17) Richmond, G. L. *Annu. Rev. Phys. Chem.* **2001**, *292*, 257.
(18) Ren, Y.; Meuse, C. W.; Hsu, S. L.; Stidham, H. D. *J. Phys. Chem.* **1994**, *98*, 8424.
(19) Willard, D. M.; Riter, R. E.; Levinger, N. E. *J. Am. Chem. Soc.* **1998**, *120*, 4151.
(20) Chamberlain, J.; Pemberton, J. E. *Langmuir* **1997**, *13*, 3074.
(21) Dluhy, R. A. *J. Phys. Chem.* **1986**, *98*, 1371.
(22) Buontempo, J. T.; Rice, S. A. *J. Chem. Phys.* **1993**, *98*, 5835.
(23) Bell, G. R.; Bain, C. D.; Ward, R. N. *J. Chem. Soc., Faraday Trans.* **1996**, *92*, 515.
(24) Knobler, C. M. *Advances in Chemical Physics*; Wiley: New York, 1990; Vol. 77.
(25) Fiehrer, K. M.; Nathanson, G. M. *J. Am. Chem. Soc.* **1997**, *119*, 251.
(26) Mitrinovic, D. M.; Zhang, Z.; Williams, S. M.; Huang, Z.; Schlossman, J. L. *J. Phys. Chem. B* **1999**, *103*, 1779.
(27) Brezesinski, G.; Thoma, M.; Struth, B.; Mohwald, H. *J. Phys. Chem.* **1996**, *100*, 3126.
(28) Lu, J. R.; Li, Z. X.; Thomas, R. K.; Penfold, J. *J. Chem. Soc., Faraday Trans.* **1996**, *92*, 403.
(29) Weinbach, S. P.; Kjaer, K.; Bouwman, W.; Als-Nielsen, J.; Leiserowitz, L. *J. Phys. Chem.* **1996**, *100*, 8356.
(30) Israelachvili, J. N. *Intermolecular and Surface Forces*; Academic Press: New York, 1996; Vol. 2.
(31) Eisenthal, K. B. *Chem. Rev.* **1996**, *96*, 1343.
(32) Wirth, M. J.; Burbage, J. D. *J. Phys. Chem.* **1992**, *96*, 9022.
(33) Shen, Y. R. *Nature* **1989**, *337*, 519.
(34) Bloembergen, N. *Opt. Acta* **1966**, *13*, 311.
(35) Corn, R. M.; Higgins, D. A. *Chem. Rev.* **1994**, *94*, 107.
(36) Richmond, G. L.; Robinson, J. M.; Shannon, V. L. *Prog. Surf. Sci.* **1988**, *28*, 1.
(37) Bloembergen, N.; Simmon, H. J.; Lee, C. H. *Phys. Rev.* **1969**, *181*, 1261.
(38) Gragson, D. E.; Richmond, G. L. *J. Chem. Phys.* **1997**, *107*, 9687.
(39) Gragson, D. E.; McCarty, B. M.; Richmond, G. L. *J. Phys. Chem.* **1996**, *100*, 14272.
(40) Gragson, D. E.; Richmond, G. L. *J. Phys. Chem. B* **1998**, *102*, 3847.
(41) Gragson, D. E.; Richmond, G. L. *J. Phys. Chem. B* **1998**, *102*, 569.
(42) Gragson, D. E.; Richmond, G. L. *J. Am. Chem. Soc.* **1998**, *120*, 366.
(43) Gragson, D. E.; McCarty, B. M.; Richmond, G. L. *J. Am. Chem. Soc.* **1997**, *119*, 6144.
(44) Goates, S. R.; Schofield, D. A.; Bain, C. D. *Langmuir* **1999**, *15*, 1400.
(45) Schreier, F. *J. Quantum Spectrosc. Radiat. Transfer* **1992**, *48*, 743.
(46) Wolfrum, K.; Laubereau, A. *Chem. Phys. Lett.* **1994**, *228*, 83.
(47) Lobau, J.; Wolfrum, K. *J. Opt. Soc. Am. B* **1997**, *14*, 2505.
(48) Hirose, C.; Akamatsu, N.; Domen, K. *Appl. Spectrosc.* **1992**, *46*, 1051.
(49) Hirose, C.; Akamatus, N.; Domen, K. *J. Chem. Phys.* **1992**, *96*, 997.
(50) Brown, M. G.; Raymond, E. A.; Allen, H. C.; Scatena, L. F.; Richmond, G. L. *J. Phys. Chem. A* **2000**, *104*, 10220.
(51) Fredkin, D. R.; Komornicki, A.; White, S. R.; Wilson, K. R. *J. Chem. Phys.* **1983**, *78*, 7077.
(52) Bain, C. D. *J. Chem. Soc., Faraday Trans.* **1995**, *91*, 1281.
(53) Yang, Y. J.; Pizzolatto, R. L.; Messmer, M. C. *J. Opt. Soc. Am. B* **2000**, *17*, 638.
(54) Conboy, J. C.; Messmer, M. C.; Richmond, G. L. *J. Phys. Chem.* **1996**, *100*, 7617.
(55) Bell, G. R.; Li, Z. X.; Bain, C. D.; Fischer, P.; Duffy, D. C. *J. Phys. Chem. B* **1998**, *102*, 9461.
(56) Messmer, M. C.; Conboy, J. C.; Richmond, G. L. *SPIE Proc.* **1995**, *2547*, 135.

(57) Messmer, M.; Conboy, J. C.; Richmond, G. L. *J. Am. Chem. Soc.* **1995**, *117*, 8039.
(58) Becraft, K.; Richmond, G. L. *Langmuir* **2001**, *17*, 7721.
(59) McKenna, C. E.; Knock, M. M.; Bain, C. D. *Langmuir* **2000**, *16*, 5853.
(60) McGuire, J. A.; Beck, W.; Wei, X.; Shen, Y. R. *Opt. Lett.* **1999**, *24*, 1877.
(61) van der Ham, E. W. M.; Vrehen, Q. H. R.; Eliel, E. R. *Opt. Lett.* **1996**, *21*, 1448.
(62) Richter, L. J.; Petralli-Mallo, T. P.; Stephenson, J. C. *Opt. Lett.* **1998**, *23*, 1594.
(63) Scatena, L. F.; Richmond, G. L. *Science* **2001**, *292*, 908.
(64) Du, Q.; Superfine, R.; Freysz, E.; Shen, Y. R. *Phys. Rev. Lett.* **1993**, *70*, 2313.
(65) Du, Q.; Freysz, E.; Shen, Y. R. *Science* **1994**, *264*, 826.
(66) Raymond, E. A.; Tarbuck, T.; Richmond, G. L. *J. Phys. Chem. B* **2002**, *106*, 2817.
(67) Allen, H. C.; Raymond, E. A.; Richmond, G. L. *J. Phys. Chem. A* **2001**, *105*, 1649.
(68) Shultz, M. J.; Schnitzer, C.; Simonelli, D.; Baldelli, S. *Int. Rev. Phys. Chem* **2000**, *19*, 123.
(69) Schnitzer, C.; Baldelli, S.; Shultz, M. J. *Chem. Phys. Lett.* **1999**, *313*, 416.
(70) Wei, X.; Shen, Y. R. *Phys. Rev. Lett.* **2001**, *86*, 4799.
(71) Scherer, J. R. In *Advances in Infrared and Raman Spectroscopy*; Clark, R. J. H., Hester, R. E., Eds.; Heyden: Philadelphia, 1978; Vol. 5, p 149.
(72) Schuster, P.; Zundel, G.; Sandorfy, C. *The Hydrogen Bond. Recent Developments in Theory and Experiment*; North-Holland, 1976; Vols. I−III.
(73) Eisenberg, D.; Kauzmann, W. *The Structure and Properties of Water*; Oxford University Press: New York, 1969.
(74) Franks, F. *Water: A Comprehensive Treatise*; Plenum Press: New York, 1972; Vol. 1.
(75) Tanford, C. *The Hydrophobic effect: Formation of Micelles and Biological Membranes*; Wiley-Interscience Publications: New York, 1973.
(76) Walrafen, G. E.; Yang, W. H.; Chu, Y. C. *ACS Symp. Ser.* **1997**, *676*, 287.
(77) Hare, D. E.; Sorenson, C. M. *J. Chem. Phys.* **1990**, *84*, 25.
(78) Buch, V.; Devlin, J. P. *J. Chem. Phys.* **1999**, *110*, 3437.
(79) Whalley, E.; Klug, D. D. *J. Chem. Phys.* **1986**, *84*, 78.
(80) Bertie, J. E.; Whalley, E. *J. Chem. Phys.* **1964**, *40*, 1637.
(81) Simonelli, D.; Baldelli, S.; Shultz, M. J. *Chem. Phys. Lett.* **1998**, *298*, 400.
(82) Schnitzer, C.; Baldelli, S.; Shultz, J. J. *J. Phys. Chem. B* **2000**, *104*, 585.
(83) Du, Q.; Freysz, R.; Shen, Y. R. *Phys. Rev. Lett.* **1994**, *72*, 238.
(84) Du, Q.; Freysz, E.; Shen, Y. R. *Am. Inst. Phys.* **1994**, 157.
(85) Huang, Z. S.; Miller, R. E. *J. Chem. Phys.* **1989**, *91*, 6613.
(86) Watts, R. O.; Reimers, J. R. *J. Chem. Phys.* **1984**, *85*, 83.
(87) Jeffrey, G. A. *An Introduction to Hydrogen Bonding*; Oxford University Press: Oxford, 1997.
(88) Scatena, L. F.; Richmond, G. L. *J. Phys. Chem. B* **2001**, *105*, 11240.
(89) Green, J. L.; Lacey, A. R.; Sceats, M. G. *Chem. Phys. Lett.* **1986**, *130*, 67.
(90) Wall, T. T.; Hornig, D. F. *J. Chem. Phys.* **1965**, *43*, 2079.
(91) Zoidis, E.; Yarwood, J.; Tassaing, T.; Danten, Y.; Besnard, M. *J. Mol. Liq.* **1995**, *64*, 197.
(92) Kint, S.; Scherer, J. R. *J. Chem. Phys.* **1978**, *69*, 1429.
(93) Devlin, P. *J. Chem. Phys.* **1986**, *90*, 1322.
(94) Wojcik, M. J.; Buch, V.; Devlin, J. P. *J. Chem. Phys.* **1993**, *99*, 2332.
(95) Morita, A.; Hynes, J. T. *Chem. Phys.* **2000**, *258*, 371.
(96) Baldelli, S.; Schnitzer, C.; Shultz, M. J. *J. Phys. Chem. B* **1997**, *101*, 4607.
(97) Coker, D. F.; Miller, R. E.; Watts, R. O. *J. Chem. Phys.* **1985**, *82*, 3554.
(98) Conrad, M. P.; Strauss, H. L. *J. Phys. Chem.* **1987**, *91*, 1668.
(99) Chang, T.-M.; Dang, L. X. *J. Chem. Phys.* **1996**, *104*, 6772.
(100) Linse, P. *J. Chem. Phys.* **1987**, *86*, 4177.
(101) Brown, M. G.; Walker, D. S.; Richmond, G. L. *J. Phys. Chem.* **2002**, *submitted*.
(102) Gragson, D. E.; Richmond, G. L. *Langmuir* **1997**, *13*, 4804.
(103) Buch, V.; Devlin, J. P. *J. Chem. Phys.* **1991**, *94*, 4091.
(104) Lied, A.; Dosch, H.; Bilgram, J. H. *Phys. Rev. Lett.* **1994**, *72*, 3554.
(105) Dosch, H.; Lied, A.; Bilgram, J. H. *Surf. Sci.* **1995**, *327*, 145.
(106) Golecki, I.; Jaccard, C. *J. Phys. C* **1978**, *11*, 4229.
(107) Furukawa, Y.; Yamamoto, M.; Jurado, T. *J. Cryst. Growth* **1987**, *82*, 655.
(108) Beaglehole, D.; Nason, D. *Surf. Sci.* **1980**, *96*, 357.
(109) Elbaum, M.; Lipson, S. G.; Dash, J. G. *J. Cryst. Growth* **1987**, *129*, 491.
(110) Wei, X.; Miranda, P. B.; Shen, Y. R. *Phys. Rev. Lett.* **2001**, *86*, 1554.
(111) Scherer, J. R.; Snyder, R. G. *J. Chem. Phys.* **1977**, *67*, 4794.
(112) Miranda, P. B.; Xu, L.; Shen, Y. R.; Salmeron, M. *Phys. Rev. Lett.* **1998**, *81*, 5876.
(113) Salmeron, M.; Bluhm, H. *Surf. Rev. Lett.* **1999**, *6*, 1275.
(114) Su, X.; Lianos, L.; Shen, Y. R.; Somorjai, G. A. *Phys. Rev. Lett.* **1998**, *80*, 1533.
(115) Yeganeh, M. S.; Dougal, S. M.; Pink, H. S. *Phys. Rev. Lett.* **1998**, *83*, 1179.
(116) Vogel, V.; Shen, Y. R. *Annu. Rev. Mater. Sci.* **1991**, *21*, 515.
(117) Miranda, P. B.; Du, Q.; Shen, Y. R. *Chem. Phys. Lett.* **1998**, *286*, 1.
(118) Walker, R. A.; Richmond, G. L. *Colloids Surf. A* **1999**, *154*, 175.
(119) Scatena, L. F.; Richmond, G. L. Submitted for publication.
(120) Zhao, X.; Ong, S.; Eisenthal, K. B. *Chem. Phys. Lett.* **1993**, *202*, 513.
(121) Richmond, G. L. *Langmuir* **1986**, *2*, 132.
(122) Corn, R. *Anal. Chem.* **1991**, *63*, 285A.
(123) Miranda, P. B.; Shen, Y. R. *J. Phys. Chem. B* **1999**, *103*, 3292.
(124) Raduge, C.; Pflumio, V.; Shen, Y. R. *Chem. Phys. Lett.* **1997**, *274*, 140.
(125) Baldelli, S.; Schnitzer, C.; Shultz, M. J.; Campbell, D. J. *J. Phys. Chem. B* **1997**, *49*, 10435.
(126) Baldelli, S.; Schnitzer, C.; Campbell, D. J.; Shultz, M. J. *J. Phys. Chem. B* **1999**, *103*-, 2789.
(127) Baldelli, S.; Schnitzer, C.; Shultz, M. J.; Campbell, D. J. *Chem. Phys. Lett.* **1998**, *287*, 143.
(128) Baldelli, S.; Schnitzer, C.; Shultz, M. J. *Chem. Phys. Lett.* **1999**, *302*, 157.
(129) Schnitzer, C.; Baldelli, S.; Campbell, D. J.; Shultz, M. J. *J. Phys. Chem. A* **1999**, *103*, 6383.
(130) Hunt, J. H.; Guyot-Sionnest, P.; Shen, Y. R. *Chem. Phys. Lett.* **1987**, *133*, 189.
(131) Guyot-Sionnest, P.; Hunt, J. H.; Shen, Y. R. *Phys. Rev. Lett.* **1987**, *59*, 1597.
(132) Wolfrum, K.; Graener, H.; Laubereau, A. *Chem. Phys. Lett.* **1993**, *214*, 41.
(133) Stanners, C. D.; Du, Q.; Chin, R. P.; Cremer, P.; Somorjai, G. A.; Shen, Y.-R. *Chem. Phys. Lett.* **1995**, *232*, 407.
(134) Braun, R.; Casson, B. D.; Bain, C. D. *Chem. Phys. Lett.* **1995**, *245*, 326.
(135) Casson, B. D.; Braun, R.; Bain, C. D. *Faraday Discuss.* **1996**, *104*, 209.
(136) Edgar, R.; Huang, J. Y.; Popovitz-Biro, R.; Kjaer, K.; Bouwman, W. G.; Howes, P. B.; Als-Nielsen, J.; Shen, Y. R.; Lahav, M.; Leiserowitz, L. *J. Phys. Chem. B* **2000**, *104*.
(137) Zhang, D.; Gutow, J.; Eisenthal, K. B. *J. Phys. Chem.* **1994**, *98*, 13729.
(138) Watry, M.; Richmond, G. L. *J. Am. Chem. Soc.* **2000**, *122*, 875.
(139) Zhuang, X.; Miranda, P. B.; Kim, D.; Shen, Y. R. *Phys. Rev. B* **1999**, *59*, 12632.
(140) Knock, M. M.; Bain, C. D. *Langmuir* **1999**, *16*, 2857.
(141) Bell, G. R.; Manning-Benson, S.; Bain, C. D. *J. Phys. Chem. B* **1998**, *102*, 218.
(142) Ward, R. N.; Duffy, D. C.; Bell, G. R.; Bain, C. D. *Mol. Phys.* **1996**, *88*, 269.
(143) Bell, G. R.; Bain, C. D.; Li, Z. X.; Thomas, R. K.; Duffy, D. C.; Penfold, J. *J. Am. Chem. Soc.* **1997**, *119*, 10227.
(144) Hoffmann, H.; Ebert, G. *Angew. Chem., Int. Ed. Engl.* **1988**, *27*, 902.
(145) Porter, M. R. *Handbook of Surfactants*; Chapman and Hall: London, 1994; Vol. 2.
(146) Sefler, G. A.; Du, Q.; Miranda, P. B.; Shen, Y. R. *Chem. Phys. Lett.* **1995**, *235*, 347.
(147) Casson, B. D.; Bain, C. D. *J. Phys. Chem. B* **1998**, *102*, 7434.
(148) Zhang, D.; Gutow, J. H.; Eisenthal, K. B. *J. Chem. Phys.* **1993**, *98*, 5099.
(149) Eisenthal, K. B. *Acc. Chem. Res.* **1993**, *26*, 636.
(150) Zhang, D.; Gutow, J. H.; Eisenthal, K. B. *J. Chem. Soc., Faraday Trans.* **1996**, *92*, 539.
(151) Huang, J. Y.; Wu, M. H. *Phys. Rev. E* **1994**, *50*, 3737.
(152) Allen, H. C.; Raymond, E. A.; Richmond, G. L. *Curr. Opin. Colloids Surf.* **2000**, *5*, 74.
(153) Allen, H. C.; Gragson, D. E.; Richmond, G. L. *J. Phys. Chem. B* **1999**, *103*, 660.
(154) Davis, D.; Chen, G.; Kasibhatla, P.; Jefferson, A.; Tanner, D.; Eisele, F.; Lenschow, D.; Neff, W.; Berresheim, H. *J. Geophys. Res.* **1998**, *103*, 1657.
(155) Jefferson, A.; Tanner, D. J.; Eisels, F. L.; David, D. D.; Chen, G.; Crawford, J.; Huey, J. W.; Torres, A. L.; Berresheim, G. *J. Geophys. Res.* **1998**, *103*, 1647.
(156) Singh, H. B.; O'Hara, D.; Herlth, D. *J. Geophys. Res.* **1994**, *99*, 1805.
(157) Yeh, Y. L.; Zhang, C.; Held, H.; Mebel, A. M.; Wei, X.; Lin, S. H.; Shen, Y. R. *J. Chem. Phys.* **2001**, *114*, 1837.
(158) Simonelli, D.; Shultz, M. J. *J. Chem. Phys.* **2000**, *112*, 6804.
(159) Harrison, R. M.; Gieken, R. v. *Atmospheric Particles*; John Wiley Sons: Chichester; New York, 1998; Vol. 5.
(160) Richmond, G. L. *Anal. Chem. News Views* **1997**, *69*, 536A.
(161) Conboy, J. C.; Messmer, M. C.; Walker, R.; Richmond, G. L. *Prog. Colloid Polym. Sci.* **1997**, *103*, 10.

(162) Conboy, J. C.; Messmer, M. C.; Richmond, G. L. *Langmuir* **1998**, *14*, 6722.
(163) Conboy, J. C.; Messmer, M. C.; Richmond, G. L. *J. Phys. Chem. B* **1997**, *101*, 6724.
(164) Mohwald, H. *Annu. Rev. Phys. Chem.* **1990**, *41*, 441.
(165) McConnell, H. M. *Annu. Rev. Phys. Chem.* **1991**, 171.
(166) Knobler, C. M.; Desai, R. C. *Annu. Rev. Phys. Chem.* **1992**, *43*, 207.
(167) Walker, R. A.; Conboy, J. C.; Richmond, G. L. *Langmuir* **1997**, *13*, 3070.
(168) Walker, R. A.; Gruetzmacher, J. A.; Richmond, G. L. *J. Am. Chem. Soc.* **1998**, *120*, 6991.
(169) Walker, R. A.; Smiley, B. L.; Richmond, G. L. *Spectroscopy* **1999**, *14*, 18.
(170) Smiley, B.; Richmond, G. L. *Biopolymers (Biospectroscopy)* **2000**, *57*, 111.
(171) Smiley, B.; Richmond, G. L. *J. Phys. Chem. B* **1999**, *103*, 653.
(172) Kim, J.; Cremer, P. S. *J. Am. Chem. Soc* **2000**, *122*, 12371.
(173) Kim, J.; Kim, G.; Cremer, P. S. *Langmuir* **2001**, *17*, 7255.
(174) Kim, J.; Cremer, P. S. *ChemPhysChem* **2001**, *8/9*, 543.
(175) Kim, G.; Gurau, M.; Kim, J.; Cremer, P. *Langmuir* **2002**, *18*, 2807.
(176) Bain, C. D.; Davies, P. B.; Ward, R. N. *Langmuir* **1994**, *10*, 2060.
(177) Ward, R. N.; Davies, P. B.; Bain, C. D. *J. Phys. Chem. B* **1997**, *101*, 1594.
(178) Briggs, A. M.; Johal, M. S.; Davies, P. B. *Langmuir* **1999**, *15*, 1817.
(179) Zolk, M.; Eisert, M.; Pipper, J.; Herrwerth, S.; Eck, W.; Buck, M.; Grunze, M. *Langmuir* **2000**, *16*, 5849.
(180) Miranda, P. B.; Pflumio, V.; Saijo, H.; Shen, Y. R. *Chem. Phys. Lett.* **1997**, *264*, 387.
(181) Duffy, D. C.; Friedmann, A.; Boggis, S. A.; Klenerman, D. *Langmuir* **1998**, *14*, 6518.
(182) Guyot-Sionnest, P.; Tadjeddine, A. *Chem. Phys. Lett.* **1990**, *172*, 341.
(183) Tadjeddine, A.; Guyot-Sionnest, P. *Electrochim. Acta* **1991**, *36*, 1849.
(184) Daum, W.; Friedrich, K. A.; Klunker, C.; Knabben, D.; Stimming, U.; Ibach, H. *Appl. Phys.* **1994**, *59*, 553.
(185) Friedrich, K. A.; Daum, W.; Klunker, C.; Knabben, D.; Stimming, U.; Ibach, H. *Surf. Sci.* **1995**, *335*, 315.
(186) Daum, W.; Dederichs, F.; Muller, J. E. *Phys. Rev. Lett.* **1998**, *80*, 766.
(187) Tadjeddine, A.; Peremans, A.; Guyot-Sionnest, P. *Surf. Sci.* **1995**, *335*, 210.
(188) Bowmaker, G. A.; Leger, J. M.; LeRille, A.; Melendres, C. A.; Tadjeddine, A. *Soc. Faraday Trans.* **1998**, *94*, 1309.
(189) LeRille, A.; Tadjeddine, A.; Zheng, W. Q.; Peremans, A. *Chem. Phys. Lett.* **1997**, *271*, 95.
(190) Ong, T. H.; Davies, P. B.; Bain, C. D. *J. Phys. Chem.* **1993**, *97*, 12047.
(191) Peremans, A.; Tadjeddine, A. *J. Chem. Phys.* **1995**, *103*, 7197.
(192) Peremans, A.; Tadjeddine, A. *Phys. Rev. Lett.* **1994**, *73*, 3010.
(193) Tadjeddine, A.; Peremans, A. *J. Chim. Phys.* **1996**, *93*, 662.
(194) Tadjeddine, A.; Peremans, A. *J. Electroanal. Chem.* **1996**, *409*, 115.
(195) Peremans, A.; Tadjeddine, A. *Chem. Phys. Lett.* **1994**, *220*, 481.
(196) Peremans, A.; Tadjeddine, A. *J. Electroanal. Chem.* **1995**, *395*, 313.
(197) Tadjeddine, A.; Peremans, A. *Surf. Sci.* **1996**, *368*, 377.
(198) Peremans, A.; Tadjeddine, A.; Guyot-Sionnest, P. *Chem. Phys. Lett.* **1995**, *247*, 243.
(199) Peremans, A.; Tadjeddine, A.; Zheng, W. Q.; LeRille, A.; Guyot-Sionnest, P.; Thiry, P. *Surf. Sci.* **1996**, *368*, 384.
(200) Schmidt, M. E.; Guyot-Sionnest, P. *J. Chem. Phys.* **1996**, *104*, 2438.
(201) Baldelli, S.; Mailhot, G.; Ross, P.; Shen, Y.-R.; Somorjai, G. A. *J. Phys. Chem. B* **2001**, *105*, 654.
(202) Dressen, L.; Humbert, C.; Hollander, P.; Mani, A. A.; Ataka, K.; Thiry, P. A.; Peremans, A. *Chem. Phys. Lett.* **2001**, *333*, 327.
(203) Gracias, D. H.; Chen, Z.; Shen, Y. R.; Somorjai, G. A. *Acc. Chem. Res.* **1999**, *32*, 930.
(204) Kim, D.; Shen, Y. R. *Appl. Phys. Lett.* **1999**, *74*, 3314.

CR0006876